Does a general relationship exist between fluorescent dissolved organic matter and microbial respiration? – The case of the dark equatorial Atlantic Ocean.

Authors:

Patricia De La Fuente[a] (patriciadlfg@icm.csic.es)

Celia Marrasé[a] (celia@icm.csic.es)

Antonio Canepa[a] (canepa@icm.csic.es)

X. Antón Álvarez-Salgado[b] (xsalgado@iim.csic.es)

Marc Gasser[a] (gasser@icm.csic.es)

Noelia M. Fajar[b] (nfajar@iim.csic.es)

Cristina Romera-Castillo[c] (cromerac@fiu.edu)

Josep L. Pelegrí[a] (pelegri@icm.csic.es)

[a] Institut de Ciències del Mar, CSIC, Passeig Maritim de la Barceloneta 37-49, 08003, Barcelona, Spain.
[b] Instituto de Investigacións Mariñas, CSIC, Eduardo Cabello, 6, 36208 Vigo, Spain.
[c] Department of Chemistry and Biochemistry, Florida International University, Miami, FL. 33199, USA.

Corresponding Author:

Celia Marrasé
Institut de Ciències del Mar, CSIC
Passeig Maritim de la Barceloneta 37- 49
08003, Barcelona, Spain.
Tel: (+34) 93 230 95 91
Fax: (+34) 93 230 95 55
Email: celia@icm.csic.es

Abstract

The distributions of humic-like fluorescent dissolved organic matter (at excitation/emission wavelengths of 340/440 nm, F(340/440)) and apparent oxygen utilization (AOU) are determined from water samples taken at 27 stations along 7.5ºN, in the equatorial Atlantic Ocean. The relationship between F(340/440) and AOU is evaluated. The influence of water mass mixing is removed through multiple regressions of both F(340/440) and AOU with salinity and temperature for the ocean interior. A general and significant relationship between the residuals of F(340/440) and AOU is found for the entire water column deeper than 200 m (R^2 = 0.79, n = 360, p-value$<$ 0.001), endorsing the idea that changes in fluorescence intensity are directly related to *in situ* oxidation of organic matter by microbial activity in the dark equatorial Atlantic Ocean. In addition, we analyse and discuss the relationships between the residuals of F(340/440) and AOU for all individual water masses.

Keywords: Water masses; Fluorescent dissolved organic matter; AOU; Equatorial Atlantic Ocean.

1. Introduction

The major source of marine dissolved organic matter (DOM) in the epipelagic ocean is the photosynthesis of phytoplankton (Hansell *et al*., 2009; Hansell, 2013; Nelson & Siegel, 2013). DOM and organic particles that escape rapid mineralization by heterotrophic microbes in the epipelagic ocean are transformed by either biotic (Microbial Carbon Pump, Jiao *et al*., 2010) or abiotic processes into recalcitrant material. Such material accumulates in the mesopelagic and bathypelagic layers to form the largest reservoir of reduced carbon on Earth (Hansell *et al*., 2009; Hansell, 2013; Nelson & Siegel, 2013).

A variable fraction of this recalcitrant material fluoresces at the excitation/emission (Ex/Em) wavelengths characteristic of humic substances (Coble *et al*., 1990; Coble, 1996, 2007) when irradiated with ultraviolet (UV) light, the so called fluorescent DOM (FDOM). In oceanic waters, the profile of humic-like FDOM is typically low at the sea surface and increases with depth (Chen & Bada, 1992; Yamashita & Tanoue, 2008; Yamashita *et al* 2010; Jørgensen *et al*., 2011). However, the fluorescence intensity is relatively high in surface waters of upwelling regions because of the enhanced biological activity and the upward flux of FDOM-rich mesopelagic waters (Determann, 1996; Nieto-Cid *et al*., 2005, 2006; Romera-Castillo *et al*., 2011a; Jørgensen *et al*., 2011; Nelson & Siegel, 2013), and in areas with large inputs of terrestrial organic matter (Del Castillo *et al*., 1999; Nelson & Siegel, 2013).

In the dark open ocean (waters deeper than 200 m, hereafter named ocean interior), because of the significant association between humic-like DOM fluorescence and apparent oxygen utilization (AOU) (Hayase *et al*., 1989; Chen & Bada, 1992; Hayase & Shinozuka, 1995; Yamashita *et al*., 2007; Yamashita & Tanoue, 2008; Yamashita et al., 2010; Jørgensen *et al*., 2011; Nelson & Siegel, 2013; Álvarez-Salgado *et al*., 2013), the humic-like FDOM serves as a tracer for the generation of recalcitrant DOM as a by-product of microbial respiration. However, it seems likely that the observed distributions of humic-like FDOM and AOU, and hence their relationship, will depend on their content at origin, typically within surface waters before they escape to the deep ocean

(Yamashita & Tanoue, 2008; Nelson & Siegel, 2013; Álvarez-Salgado *et al*., 2013).

The MOC2-Equatorial cruise occupied a transatlantic line along 7.5ºN in April-May 2010 on board the R/V *Hespérides*. The meridional transport of properties across the 7.5ºN line (*i.e*. heat, fresh water, carbon and nutrients among others) has been previously studied by several authors (Fuglister, 1960; Oudot, 1993; Arhan *et al*., 1998; Lappo *et al*., 2001; Sarafanov *et al*., 2007). This transect constitutes a meeting zone for waters of northern and southern origin at all levels. Western boundary currents are responsible for inter-hemispheric exchange, most of the time after substantial recirculations within the equatorial and tropical regions. The net flow in the epipelagic (0–200 m) and mesopelagic (200–1000 m) layers is northward, being compensated by a net southward transport in the abyssal ocean, from 1000 m to the bottom (Arhan *et al*., 1998; Stramma & Schott, 1999).

The mesopelagic layer is formed by central (upper thermocline) and intermediate waters, while the abyssal ocean (here defined as waters deeper than 1000 m) is dominated by deep and bottom waters. In the central waters domain we find a combination of North Atlantic Central Water (NACW) and South Atlantic Central Water (SACW), with a predominance of relatively aged SACW. At the intermediate levels the northward extension of Antarctic Intermediate Water (AAIW) occurs and at depth the North Atlantic Deep Water (NADW) overlays the Antarctic Bottom Water (AABW).

Field observations of humic-like FDOM in the equatorial Atlantic Ocean are scarce, predominantly sampled along meridional transects close to the African coast (Determann, 1996; Jørgensen *et al*., 2011; Nelson & Siegel, 2013;

Andrew *et al*., 2013). Therefore, the humic-like FDOM data obtained during the MOC2-Equatorial cruise, with good spatial resolution across the under-sampled equatorial Atlantic Ocean, provides an excellent opportunity to evaluate the relative influence of both FDOM-concentration at origin and *in situ* microbial activity on the observed humic-like FDOM distribution. Specifically, the spatial distribution of FDOM (with Ex/Em wavelengths of 340/440 nm) is used as a proxy for recalcitrant dissolved organic matter within the equatorial Atlantic Ocean, and the dependence of this variable with AOU (as a proxy for microbial respiration) is examined. We indeed find that the relationship between humic-like FDOM and AOU changes among the different water strata. Therefore, we use salinity and temperature, which are characteristic of each water mass, to remove the effect of the different initial concentrations. After applying the best fit-model to explain the dependence of FDOM and AOU on temperature and salinity, we examine the behaviour of both FDOM and AOU residuals. These residuals display a general significant relationship for the ocean interior, which endorses the very important role of *in situ* microbial processes in relation to the Microbial Carbon Pump (MCP) and recalcitrant DOM storage in the dark equatorial Atlantic Ocean (Jiao *et al*., 2010).

2. Material and methods

2.1 Measurements

The second phase of the MOC2-Equatorial cruise crossed the equatorial Atlantic Ocean from South America to West Africa along 7.5ºN, between 20 April and 13 May 2010, with a total of 62 hydrographic stations. Measurements for this study were obtained from 27 stations along this track (Fig. 1), using water samples from the whole water column (except for stations 63, 72, 108 and 109 where the deepest samples were taken at 99 m, 153 m, 1570 m and 181 m, respectively). Vertical profiles of temperature and conductivity were obtained with a SeaBird 911 Plus CTD system mounted in a 24 Niskin bottle rosette that collected water samples at standard depths; Chl-a fluorescence was determined with a Seapoint Fluorometer sensor.

Seawater samples for the O_2 analysis were taken from Niskin bottles in sealed flasks (~250 mL) with a PVC pipe avoiding the bubble formation and stored in darkness for 24 hours. Dissolved oxygen concentration was measured using an automated potentiometric modification of the original Winkler method following WOCE standards (WOCE, 1994). The accuracy of the method is $\pm$ 0.5 μmol kg^{-1}.

Water samples for the FDOM measurements were collected from each Niskin bottle in acid cleaned glass bottles of 250 mL, previously rinsed three times with the corresponding seawater. In order to avoid sample contamination, several precautions were taken during collection of the water sample: gloves were used, contact with the spigot of the Niskin bottle was avoided, and the formation of air bubbles was minimized. Each sample was stored in darkness and far away from the presence of volatile organic compounds. They were allowed to stand until reaching room temperature. Fluorescence measurements were conducted within two hours after sampling; samples were not filtered.

Fluorescence measurements were performed using a Perkin Elmer LS spectrometer with a 150 W Xenon lamp, and the sensitivity mode was set at 10-nm slit widths for both excitation and emission wavelengths. Milli-Q water was used as a reference blank for fluorescence analysis. An acid-cleaned quartz cell of 1 cm was rinsed three times with the sample and then fluorescence intensity was measured at fixed Ex/Em wavelengths of 340/440 nm (F(340/440)), which is characteristic of humic-like substances (Coble et al.,1990; Coble,1996). F(340/440) data was normalized to Raman Units (R.U.) according to Lawaetz & Stedmon (2009).

AOU is defined as the difference between saturation O_2 concentration ($O_{2,sat}$), which depends on *in situ* temperature and salinity and the observed O_2 concentration, *i.e*. AOU = $O_{2,sat}$ – O_2 (Weiss, 1970; Ito *et al*., 2004); $O_{2,sat}$ was calculated following Benson & Krause (1984).

2.2 Water regions and water masses

The water column is divided into surface (0 - 200 m) and ocean interior (deeper than 200 m). Furthermore, the ocean interior is separated in two depth-layers: mesopelagic (200 - 1000 m) and abyssal (1000 m to the sea bottom). It is also classified into different water masses using neutral density levels, following the study of San Antolín *et al*., (2012) for the same section. Neutral density, γ^n, is computed following Jackett & McDougall (1997) using the code available at the Gibbs-SeaWater (GSW) Oceanographic Toolbox (McDougall & Barker, 2011) with the anomaly values defined as neutral density = (1000 + γ^n) kg m^{-3}. In the mesopelagic layer we find central waters (NACW and SACW), with a neutral density range of $26.65 < \gamma^n < 27.3$, and intermediate waters (AAIW), with a neutral density range of $27.30 < \gamma^n < 27.8$. The abyssal layer is occupied by deep waters (NADW), with neutral densities of $27.8 < \gamma^n < 28.12$, and bottom waters (AABW), with neutral densities of $\gamma^n > 28.12$.

Water masses in the equatorial Atlantic Ocean are characterized on the basis of potential temperature (θ), salinity (S), and dissolved oxygen (O_2) (Figs. 2 and 3). The predominant central water along 7.5ºN is SACW, having its origin in the southern hemisphere (Stramma & Schott, 1999). Below 200 m, SACW is characterized by θ and S values that define a straight line in the (θ, S) space, which passes through points (6ºC, 34.6) and (14ºC, 35.4) (Fig. 3d). SACW shows an oxygen minimum at 300 – 500 m in the eastern region which is indicative of weak water renewal near the Guinea Dome region (Stramma & Schott, 1999) (Figs. 2 and 3). AAIW appears as a cold and low-salinity tongue at depths 500 – 1100 m, most pronounced in the western half of the 7.5ºN section (Stramma & Schott, 1998; Arhan *et al*., 1998; Sarafanov *et al*., 2007; Machín & Pelegrí, 2009) (Figs. 2 and 3). NADW stands out as a high-salinity and oxygen-rich domain; NADW is commonly divided into three components: upper NADW (UNADW), recognizable by a mid-depth salinity maximum, and middle and lower NADW (MNADW, LNADW), most distinguishable by oxygen maxima at 2000–2500 m and approximately 3700 m, respectively (Figs. 2 and 3) (Arhan *et al*., 1998; Sarafanov *et al*., 2007; Talley *et al*., 2011). The lowest temperature values are found in the AABW (Arhan *et al*., 1998; Sarafanov *et al*., 2007; Lappo *et al*., 2001) (Figs. 2 and 3). AABW is a mixture of unventilated Lower Circumpolar Deep Water (LCDW) and Weddell Sea Deep Water (WSDW), the latter being oxygen-rich cold waters recently formed in the Antarctic margins (Orsi et *al*., 1999); AABW presents salinity and oxygen concentrations lower than NADW (Figs. 2 and 3), characteristic of its southern origin (Arhan *et al*., 1998; Lappo *et al*., 2001).

2.3 Statistical analysis

The linear relationships between F(340/440) and AOU are evaluated separately for the surface ocean (0-200 m) and for the ocean interior (> 200 m). For the ocean interior, individual linear relationships between F(340/440) and AOU are also obtained for the four water strata (central, intermediate, deep and bottom). Model II linear regression is used to examine the relationship between F(340/440) and AOU; model II regression refers to a family of model-fitting procedures that acknowledge the uncertainty of both response and predictor variables (Logan, 2010). Among different techniques, the Standard (Reduced) Major Axis (SMA) is selected. SMA arranges the variables in a dimensionally homogeneous way prior to the regression analysis (Legendre & Legendre, 1998). The uncertainty of response and predictor variables are incorporated through the minimization of the sum squares of the triangular areas defined by the observations and the regression line (Logan, 2010). The coefficients (intercept and slope) with their respective standard deviations obtained from the linear relationships, together with the corresponding correlation coefficient (R^2) and p-value (α = 0.05), are shown in Table 1.

To determine the relationship between F(340/440) and AOU for the ocean interior without the influence of temperature and salinity, as a proxy of water masses, we follow two steps. The first step consists on performing multiple non-linear regressions for both F(340/440) and AOU as a function of temperature and salinity over the whole (θ, S) space. A non-linear response is included in the models in the form of θ and S quadratic and interaction terms. The models turn out to have good skill capturing the variability associated to the (θ, S) pair of values, *i.e*. related to the source water masses. The optimal models are established based on the Akaike's Information Criterion (AIC) (data not shown).

The AIC method penalizes in a negative way the excess of parameters, so it prevents an over-parameterization and allows evaluating which model gives the best fit: the lower the AIC value the better is the model (Zuur *et al*., 2009). For the optimal models, the regression coefficient (R^2) and the p-value ($\alpha = 0.05$) are shown.

The rationale behind searching for a relation between either F(340/440) or AOU with temperature and salinity, is that these latter variables have proved to be a good proxy for different water masses (Mamayev, 1975). Water masses are often characterized by their conservative thermohaline properties. Non-conservative parameters are influenced not only by physical mixing and advection, but also by biological processes. Earlier studies have removed the physical variability (assumed to be associated with θ and S) through local linear regression models on salinity and temperature; these models are local in the sense that a (θ, S) pair is to be attained by the linear mixing in the (θ, S) space of up to a maximum of three end-member water types (Castro *et al*., 2006; Carlson *et al*., 2010). The non-linear method proposed here takes into account the possibility of non-isotropic mixing by incorporating the non-linear dependences with temperature and salinity.

The second step consists on subtracting the values estimated from the (θ, S) pair through the optimal model from the observed values. These residuals contain the FDOM and AOU variability not explained by (θ, S), and they are expected to mainly reflect the biological activity (Castro *et al*., 2006; Carlson *et al*., 2010). Henceforth we will refer to them as F(340/440) and AOU biological anomalies, with the notation ΔF(340/440) and ΔAOU respectively. For each water stratum, the relationship between ΔF(340/440) and ΔAOU is evaluated through a model II analysis of covariance (ANCOVA) using the package “smatr” (Warton *et al*., 2012) (Table 2). Finally, a simple model II (SMA) linear relationship between ΔF(340/440) and ΔAOU for the entire ocean interior is obtained. The calculated relationship is evaluated through the correlation coefficient (R^2), and the significance p-value (α = 0.05).

All statistical analyses are done using the free statistical software R, version 2.15.2 (R Core Developmental Team, 2012), and the computing environment Matlab v.7.6.0 (R2008a).

3. Results and discussion

3.1 F(340/440) and AOU distributions

3.1.1 Surface (0 – 200 m)

F(340/440) values are lowest in the first meters of the water column probably due to photobleaching by UV and blue light (Mopper *et al*., 1991; Chen & Bada, 1992; Stedmon & Markager, 2005). The intensity of sunlight, which is very high, and the stability of the near-surface layer at this latitude favour the photodegradation of FDOM (Determann, 1996; Chen & Bada, 1992; Mopper *et al*., 1991). The range of F(340/440) values is very narrow throughout the entire 7.5ºN section (2 to 3 $\times10^{-3}$ R.U.). In surface waters the highest F(340/440) values were found in stations 50 and 109 (7 $\times10^{-3}$ R.U. and 5 $\times10^{-3}$ R.U., respectively). The high surface F(340/440) value at station 50 coincides with a low sea-surface salinity of 34.84, evidencing the influence of the Amazon plume (Salisbury *et al*., 2011). The high value observed in station 109 may indicate a terrestrial source (Del Castillo *et al*., 1999), as this is the station nearest to the African coast. The depth limit at which F(340/440) values remain low (<5 $\times10^{-3}$

R.U.) decreases from West to East (54 ±10 m to 6 ±0.8 m) (Fig. 4) due to the eastward uplift of the seasonal thermocline. Below this depth, the F(340/440) signal increases rapidly with depth (Figs. 4a and 5a).

F(340/440) presents a subsurface maximum in the upper part of the main thermocline, close to the deep chlorophyll maximum (DCM) and coincident with a strong depth gradient in AOU (Figs. 4 and 5), therefore suggesting biological *in situ* FDOM production. The depths of F(340/440) and Chl-a maxima in the westernmost stations vary from 120 to 200 m (Fig.4a) and from 70 to 100 m (Fig. 4b), respectively. At the easternmost stations, maximum values take place at 40-50 m for both variables (Fig.4). The sub-surface F(340/440) maximum fluorescence intensities remain in a narrow range of 9–10 $\times 10^{-3}$ R.U. in the western part of the section, stations 50 to 98 (Fig. 4a). For stations 101 to 109, in the eastern end of the section, the F(340/440) and DCM sub-surface maxima show the highest values, with mean values of 13 ± 1.4 $\times 10^{-3}$ R.U. for F(340/440) and 0.90 ±0.22 mg/m^3 for Chl-a (Fig. 4), probably related to the influence of upwelling near the Guinea Dome (Siedler *et al.*, 1992).

3.1.2 Ocean interior (deeper than 200 m)

Through the mesopelagic layer (200–1000 m), F(340/440) remains approximately constant but displays significant zonal changes, with maximum values in the eastern region. The distribution of AOU also shows a substantial zonal gradient, but most remarkably it typically displays a prominent depth maximum at 400–500 m (Figs. 5 and 6). The maximum F(340/440) and AOU values correspond to the eastern part of the section (Figs. 5 and 6), where

Guinea Dome upwelling takes place and the Oxygen Minimum Zone (OMZ) is found (Arhan *et al*., 1998; Karstensen *et al*., 2008; Stramma, 2008).

The F(340/440) distribution at the mesopelagic layer displays some peaks of relatively high fluorescence intensity. The characteristic depth of these peaks ranges between 300 and 800 m, coincident with the range where maximum AOU values are found for the ocean interior (Figs. 5 and 6). This suggests a link between F(340/440) and biological activity, as other authors have pointed out (Yamashita *et al*., 2010; Jørgensen *et al*., 2011).

In the abyssal layer (1000 m to sea bottom), the vertical distribution of F(340/440) remains quite constant (Figs. 5a and 6a). The highest values of fluorescence intensity are found again in the eastern part of the section probably due to the oxidation of the downward flux of organic matter caused by upwelling near the Guinea Dome. The AOU decreases progressively from maximum values at about 500 m to minimum levels at about 2000 m, and remains approximately constant further deep.

3.2 F(340/440) – AOU relationship

3.2.1 Surface (0 – 200 m)

The significant linear relationship between F(340/440) and AOU found for the top 200 m (Slope = 5.41 (±0.17) $\times$ 10^{-5} (R.U.), R^2 = 0.83, n = 170, p-value $<$ 0.001, Table 1) suggests a biological *in situ* production of F(340/440), possibly related to the mineralization of organic matter by marine bacteria. However, this relationship should be taken with caution as there are other processes that may influence the observed values of fluorescence intensity, *i.e*. photo-degradation (Determann, 1996; Chen & Bada, 1992; Mopper *et al*., 1991) or the production of FDOM by marine phytoplankton (Romera-Castillo *et al*., 2010). Furthermore, the production of O_2 during primary production will also influence the F(340/440)-AOU relationship.

3.2.2 *Ocean interior (deeper than 200 m)*

The linear relationship between AOU and F(340/440) for the ocean interior is very weak although significant (Slope = 1.20 (±0.01)$\times$ 10^{-5} (R.U.), R^2 = 0.05, n = 360, p-value $<$ 0.001, Table 1). This weak dependence is consistent with the observed different distributions of F(340/440) and AOU across distinct water strata (Fig. 7). A scatter plot of F(340/440) as a function of AOU indeed suggests a changing dependence for the different water strata (Fig. 8a). On the light of those results, we examine the dependence of F(340/440) with AOU separately for different water strata.

Mesopelagic layer (200 – 1000 m); central and intermediate waters

The relationship of F(340/440) with AOU within the central waters is strong and significant (Slope = 3.07 (±0.14) $\times$ 10^{-5} (R.U.), R^2 = 0.81, n = 131, p-value $<$ 0.001, Table 1) and intermediate waters present a very weak but significant linear relationship (Slope = 1.85 (±0.22) $\times$ 10^{-5} (R.U.), R^2 = 0.07, n = 102, p-value < 0.05, Table 1). In the boundary between the mesopelagic and abyssal layers (900–1200 m), the AOU decreases rapidly without an equivalent change in fluorescence intensity (Figs. 5 and 6), therefore the linearity in the relationship is lost (Fig. 8a). The sharp decrease in AOU values may be due to the presence of O_2-rich upper deep waters (Fig.7b). When we only consider data in the upper part of the intermediate waters range (27.3 < γ^n < ~27.5, approximately a depth range of 500–900 m), the linear relation between

F(340/440) and AOU is high (Slope = 3.70 (±0.16) × 10^{-5} (R.U.), R^2 = 0.88, n = 66, p-value < 0.001). These results are in agreement with Yamashita & Tanoue (2008), which reported that the mesopelagic layer was the main site for production of FDOM by microbial respiration in the ocean interior.

Abyssal layer (1000 m – sea bottom); deep and bottom waters

For deep waters (27.8 < γ^n < 28.12), a weak but positive linear relationship is found between F(340/440) and AOU (Slope = 3.60 (±0.31) × 10^{-5} (R.U.), R^2 = 0.27, n = 126, p-value < 0.001, Table 1); bottom waters (γ^n > 28.12) do not present any significant linear relationship (R^2 < 0.01, n = 30, p-value = 0.81, Table 1). Both deep and bottom waters show relatively high values of F(340/440) associated with AOU values lower than expected if humic-like FDOM came only from *in situ* production (Fig.8a). The high-latitude North Atlantic region, where NADW is formed each winter, is a region of high spring primary production (Ducklow & Harris, 1993) which also receives large amounts of terrestrial organic matter from the Arctic rivers (Álvarez-Salgado *et al*., 2013; Jørgensen *et al*., 2011; Dittmar & Kattner, 2003). All over, these water masses introduce high levels of O_2 and humic-like FDOM into the deep equatorial Atlantic Ocean. Respect to the AABW, a plausible explanation for the relative high FDOM/AOU ratio is linked to the conditions in those formation regions located near the Antarctic continental margin. A large fraction of recalcitrant DOM moves up to the surface, mainly in the Southern Ocean via the upwelling of NADW (Chen, 2011). This, together with low light incidence and the high depth of the surface mixed layer in this region (Siegel *et al*., 2002), results in CDOM-rich (and therefore FDOM-rich) surface waters.

3.3 FDOM and AOU residuals (ΔF(340/440), ΔAOU)

3.3.1 Non – linear models.

A significant relationship between deep humic-like FDOM (Coble's M-peak) and AOU has been reported by Yamashita & Tanoue (2008) for the Pacific Ocean basin. They found a positive and strong linear FDOM – AOU correlations for all water masses within the mesopelagic layer but with substantial differences in slope and intercept. Such differences were associated to the mixing of source waters with different initial levels of FDOM. In order to evaluate the *in situ* production rate of FDOM from the respiration rate, Yamashita & Tanoue (2008) considered only the FDOM – AOU linear relationship in the abyssal layer (>1000 m) where one single dominant water mass is found (Slope = 0.0047 [N.FI.U.], R^2 = 0.85, n=210, p-value < 0.001). Yamashita *et al*., (2010), using Fluorescence Excitation Emission Matrix (EEM) spectroscopy and multivariate data analysis Parallel Factor (PARAFAC), found a humic-like component similar to that traditionally assigned to terrestrial humic-like fluorophore (C-peak). They showed that C-peak and AOU were linearly correlated in both the mesopelagic (200 - 1000 m) and bathypelagic (1000 - 4000 m) layers. Taking into account the mixing of waters with different source in the mesopelagic layer of the Pacific Ocean, the authors only discussed the FDOM-AOU relationship in the bathypelagic layer (Slope = 0.0029 [Q.S.U.], R^2 = 0.89, n=16, p-value < 0.001). Jørgensen *et al*. (2011), found a significant relationship between component 1 (the humic–like FDOM component associated to C-peak) and AOU for the dark global ocean excluding waters from the North Atlantic (O_2 and humic-FDOM rich in origin) (Slope = 3.493×10^{-5}

(R.U.), $R^2 = 0.72$, $p < 0.05$). However, as in previous studies (Yamashita & Tanoue, 2008; Yamashita *et al.*, 2010), the variability related to the different concentrations at origin was not considered. Álvarez–Salgado *et al*. (2013) found a strong relationship between marine humic-like FDOM (Coble's M-peak) and AOU (Slope = 0.009±0.002 (QSU), $R^2 = 0.83$, n = 9, $p < 0.001$) in the deep Northern North Atlantic, but the Denmark Strait overflow water (DSOW), initially rich in O_2 and remarkable high in humic-FDOM content, was also omitted because it deviated from the general trend.

Our results (Section 3.2) show a significant but weak relationship between F(340/440) and AOU (Slope = 1.20 (±0.01) $\times 10^{-5}$ (R.U.), $R^2 = 0.05$, n = 360, p-value < 0.001, Table 1) for the dark equatorial Atlantic (> 200 m). The presence of deep and bottom waters, rich in humic-like FDOM and low in AOU at origin, would explain the weak F(340/440) – AOU relationship for the ocean interior. This is consistent with reports for the Atlantic Ocean (Jørgensen *et al.,* 2011; Álvarez-Salgado *et al.,* 2013; Nelson & Siegel, 2013*)* which point at a dependence of both F(340/440) and AOU values on the conditions where the different water masses were formed.

In order to remove the variability associated to the distinct F(340/440) and AOU "initial" conditions of each water mass, a multiple non-linear regression has been carried out between either F(340/440) or AOU with salinity and temperature (Eqs. 1 and 2); the underlying premise is that a water mass is identified by a point, or region, in the temperature-salinity space. The results show that only a small portion of the F(340/440) variability is explained by temperature and salinity ($R^2= 0.21$, p-value < 0.05; Eq. 1); instead, the AOU distribution is highly dependent on temperature and salinity, with an R^2 = 0.89 and p-value $<$ 0.001 (Eq. 2):

$$F(340/440) = -14.1 + 0.8 \times S - 1.2\times10^{-2} \times S^2 - 5.4\times10^{-2} \times \theta - 4.0\times10^{-5} \times \theta^2 + \quad (1)$$
$$+1.6\times10^{-3} \times S \times \theta + \Delta F(340/440),$$

R^2=0.20, n=369, $p < 0.001$.

$$AOU = -5.8\times10^5 + 3.4\times10^4 \times S - 502 \times S^2 - 2438 \times \theta - 2.0 \times \theta^2 + \quad (2)$$
$$+ 71.0 \times S \times \theta + \Delta AOU,$$

R^2=0.89, n=369, $p < 0.001$.

The residuals (ΔF(340/440) and ΔAOU), as deduced after subtracting the values estimated through the optimal model (Eqs. 1 and 2) from the observed values, represent the variability of F(340/440) and AOU that is not explained by temperature and salinity. The significant relationship between AOU with salinity and temperature (Eq. 2) indeed leads to an important reduction in the ΔAOU standard deviation ($SD_{\Delta AOU}$ = 17.8 µmol kg^{-1}), as compared with the AOU standard deviation (SD_{AOU} = 52.8 µmol kg^{-1}). The major reduction is observed for intermediate (SD_{AOU} = 26.4 µmol kg^{-1} versus $SD_{\Delta AOU}$ = 16.0 µmol kg^{-1}), deep (SD_{AOU} = 10.6 µmol kg^{-1} versus $SD_{\Delta AOU}$ = 7.8 µmol kg^{-1}) and bottom waters (SD_{AOU} = 10.3 µmol kg^{-1} versus $SD_{\Delta AOU}$ = 4.8 µmol kg^{-1}) and it is minimal for central waters (SD_{AOU} = 27.5 µmol kg^{-1} versus $SD_{\Delta AOU}$= 28.4 µmol kg^{-1}).

In contrast, the standard deviation of ΔF(340/440) for the ocean interior ($SD_{\Delta F(340/440)}$ = 5.7$\times10^{-4}$ R.U.) only shows a slight reduction when compared with the standard deviation of the F(340/440) data ($SD_{F(340/440)}$ = 6.4 $\times10^{-4}$ R.U.).

Such a result confirms the relatively low dependence of F(340/440) on salinity and temperature through all water strata (Eq. 1). As the FDOM residuals represent the major source of the F(340/440) variability, we can conclude that *in situ* processes have an important role in FDOM production.

A remarkable result is the low FDOM variability explained by temperature and salinity, as compared with AOU. Figure 5 shows that both AOU and F(340/440) have a noteworthy west-east gradient, not present in the salinity and potential temperature profiles (Fig. 3). In contrast, AOU presents much more depth variability than F(340/440), which correlates well with the salinity and potential temperature vertical profiles. We have no conclusive explanation for these differences, but they clearly reflect that F(340/440) is much less correlated to the water masses than AOU, which is strongly dependent on the temperature-dependent O_2 content at origin.

3.3.2 A general ΔF(340/440) - ΔAOU relationship for the ocean interior

The distributions of residuals ΔF(340/440) and ΔAOU along 7.5ºN do follow similar patterns (Fig. 9). This fact suggests that the variability of ΔF(340/440) (Fig. 9a) is associated with the variability of ΔAOU (Fig. 9b) and endorses the idea of a clear relationship between ΔF(340/440) and ΔAOU for the ocean interior.

Our results indeed show a significant, positive and high ΔF(340/440) - ΔAOU relationship for this particular area when considering the full dataset below 200 m, *i.e*. when considering all water masses present in the zone of study (Eq. 3, Fig. 8b):

$$\Delta F(340/440) = 3.14\ (\pm 0.08) \times 10^{-5} \times \Delta AOU\ , \qquad (3)$$

R^2=0.79, n=360, p < 0.001.

This significant general relationship points a biological oxidation of organic matter by microbial activity as the main source of F(340/440) in the dark ocean.

Despite the existence of this general relationship, the correlation between ΔF(340/440) - ΔAOU changes among the different water strata. Model II covariance analysis (Table 2) shows a ΔF(340/440) - ΔAOU linear relationship higher for central (R^2 = 0.92, p-value < 0.001) and intermediate waters (R^2 = 0.79, p-value < 0.001) than for deep (R^2 = 0.57, p-value < 0.001) and bottom waters (R^2 = 0.2, p-value < 0.05) (Table 2). The slopes for the linear relationships change significantly among different water strata (r_3 = 89.93, p-value < 0.001), except between central and intermediate waters (p-value= 0.71).

Furthermore, with the exception of the intermediate waters, for each water stratum the slope of the linear relationship differs significantly from the general slope, 3.14 (±0.08)$\times 10^{-5}$ (r_4 = 89.93, p-value < 0.001): p-value < 0.05 for central waters, < 0.001 for deep waters and < 0.001 for bottom waters, while p-value = 0.58 for intermediate waters (Table 2). The slope of the deep and bottom waters is indeed substantially larger than for central and intermediate waters, and also larger than the slope of the general trend (Eq. 3).

Our results agree qualitatively with those obtained by Álvarez-Salgado *et al*. (2013) for the northern North Atlantic Ocean. These authors justified the different slopes of the humic-like FDOM – AOU relationships in terms of the ventilation of the corresponding water mass realms. According to Álvarez-Salgado *et al*. (2013), during deep water formation, freshly produced organic matter is injected below the main thermocline acting as a source of DOM for bacteria in the abyssal layer. A similar result was found by Nelson *et al*., (2007, 2010) for CDOM in the Atlantic Ocean. These authors suggested that rapid formation and advection of NADW masks the existence of a high-correlation between CDOM and AOU. As F(340/440) is closely related to CDOM, the high rate of NADW and AABW ventilation could also mask the ΔF(340/440) - ΔAOU relationship found in the present study. For bottom waters, an additional source of ΔF(340/440) could come from the sediments, caused by the current-induced resuspension (Lappo *et al*., 2001; Nelson *et al*., 2007).

Considering the statistical significance of the ΔF(340/440) - ΔAOU relationship (R^2=0.79, p-value < 0.001), the fact that the Apparent Oxygen Utilization (AOU) is widely used to infer respiration in the oceans and that the variability associated to θ and S was subtracted before the analysis, this correlation could indicate that the major source of F(340/440) in the equatorial Atlantic dark ocean could be related to *in situ* biological oxidation of organic matter by microbial activity. This is particularly relevant as there are other FDOM possible sources, as mentioned in previous studies. Jørgensen *et al*. (2011) speculated that FDOM can be produced abiotically via extracellular precursors released not only by microbial activity but also through viral lysis and grazing activities among others. Recently, Andrew *et al*. (2013) suggested that chemical or microbial modification of an existing terrestrial source material could be also an importance source of humic-like FDOM. However it has been shown that C-peak, traditionally assigned with a terrestrial origin can be also produced by marine bacterial activity (Romera-Castillo *et al*., 2011b, Shimotori *et al.,* 2012) and that terrestrial material is not necessary to generate FDOM (for example, marine bacteria cultivated in artificial sea water with glucose and inorganic nutrients can produce C-peak FDOM, Kramer & Herndl (2004)).

Finally, when comparing our results with earlier works, an important issue to take into account is the differences in definitions and units for the humic-like fluorescence. Yamashita & Tanoue (2008) and Álvarez-Salgado *et al*. (2013) studied the fluorescence intensity at Ex/Em 320/420 nm, *i.e*., what Coble (1996) defined as the peak M characteristic of marine humic-like substances. Jørgensen *et al*. (2011) and Yamashita et al., 2010 obtained Ex/Em matrices instead of Ex/Em pairs and used PARAFAC modelling to define fluorescent components.

4. Conclusions

The observed distributions of F(340/440) and AOU along the 7.5ºN section complement early results for this region (Determann, 1996; Karstensen *et al*., 2008; Jørgensen *et al*., 2011) and in other ocean basins (Yamashita & Tanoue, 2008; Yamashita et al., 2010). For the ocean interior (> 200 m), the F(340/440) and AOU distributions share some similarities, but also substantial differences, particularly within the deep and bottom waters which are O_2 and humic-FDOM rich at origin. As a result we find a significant but very weak relationship between F(340/440) and AOU.

A multiple non-linear regression analysis for the ocean interior shows that more than 80% of the AOU variability along the 7.5ºN Atlantic cross section may be explained by the hydrographic characteristics, with temperature and salinity as a proxy of water masses. However, only 20% of the variability of fluorescence intensity is explained by these hydrographical characteristics. We use optimal non-linear models, for both F(340/440) and AOU as a function of temperature and salinity, in order to remove the variability associated to the water masses. Then, a general and significant relationship is found between the residuals ΔF(340/440) and ΔAOU, with a slope of 3.14 (±0.08)$\times10^{-5}$ (R.U.) (R^2 = 0.79, p-value < 0.001). This relationship is obtained using the full dataset below 200 m, *i.e.*, considering all water masses present in the zone of study regardless of the mixture of waters with different levels of preformed FDOM and AOU. This is a remarkable result because, until now, a strong and significant FDOM – AOU association has been found for the Atlantic Ocean only when omitting those waters that are O_2 and humic-FDOM rich at origin (Álvarez-Salgado *et al*., 2013; Jørgensen *et al*., 2011; Nelson & Siegel, 2013).

Despite the existence of such a significant general relationship, we still find significant differences among individual water strata. In particular, within the deep and bottom waters the production of F(340/440) associated to oxidation or organic matter appears to be higher than for central and intermediate waters. This seems to be mainly related with the ventilation of water masses but may also reflect the existence of different processes and transformations in each individual stratum.

The strong and significant general relationship between ΔF(340/440) and ΔAOU reveals that 79% of the ΔF(340/440) variability is associated to ΔAOU for the interior equatorial Atlantic Ocean. This result endorses the idea that, after removing the potential differences at origin, the major source of F(340/440) in the dark ocean is the *in situ* biological oxidation of organic matter by microbial activity.

Acknowledgments

The MOC2-Equatorial cruise was carried out with the R/V *Hespérides*, we are happy to acknowledge support by the crew and on board technicians. Funding comes from the Spanish government through MOC2 (CTM2008-06438-CO2), TIC-MOC (CTM2011-28867), DOREMI (CTM2012-34294) projects of the R+D Spanish research program and from the ECLIPSE project financed by Total Foundation. P. De La Fuente would like to thank the Agència de Gestió d'Ajuts Universitaris i de Recerca de la Generalitat de Catalunya (AGAUR) for their financial support through a FI-AGAUR fellowship. A. Canepa was funded by CONICYT (PFCHA/Doctorado al Extranjero 4a Convocatoria, 72120016). C. Romera-Castillo was funded by a Beatriu de Pinós post-doctoral fellowship from the AGAUR of the Generalitat de Catalunya. Images 2, 4, 6 and 9 have been created using Ocean Data View (R. Schlitzer, 2011, http://odv.awi.de).

References

Álvarez-Salgado, X. A., Nieto-Cid, M., Álvarez, M., Pérez, F. F., Morin, P., and Mercier, H., 2013. New insights on the mineralization of dissolved organic matter in central, intermediate, and deep-water masses of the northeast North Atlantic. Limnol. Oceanogr, 58(2), 2013, 681–696. doi:10.4319/lo.2013.58.2.0000.

Andrew, A. A., Del Vecchio, R., Subramaniam, A., and N. V.Blough 2013. Chromophoric dissolved organic matter (CDOM) in the Equatorial Atlantic Ocean: Optical proper-ties and their relation to CDOM structure and source. Mar.Chem. 148: 33-43, 10.1016/j.marchem.2012.11.001.

Arhan, M., Mercier, H., Bourlès, B., Gouriou, Y., 1998. Hydrographic sections across the Atlantic at 7^{o}30N and 4^{o}30S. Deep-Sea Research I, 45, 829-872.

Benson, B.B., and Krause, D.,Jr., 1984. The Concentration and Isotopic Fractionation of Oxygen Dissolved in Freshwater and Seawater in Equilibrium with the Atmosphere. Limnology and Oceanography, 29, 3, 620–632, 1984.

Carlson, C. A., and others. 2010. Dissolved organic carbon export and subsequent remineralization in the mesopelagic and bathypelagic realms of the North Atlantic basin. Deep-Sea Res. Part II 57: 1433–1445, doi:10.1016/j.dsr2.2010.02.013

Castro, C. G., Nieto-Cid, M., Álvarez-Salgado, X.A., and Pérez, F. F., 2006. Local remineralization patterns in the mesopelagic zone of the eastern North Atlantic, off the NW Iberian Peninsula. Deep-Sea Res. Part I 53: 1925–1940.

Chen, C. T. A. Microbial carbon pump: additional considerations. Nature Rev. Microbiol. 31 May 2011 (doi: 10.1038/nrmicro2386-c4).

Chen, R.F., Bada, J.L., 1992. The fluorescence of dissolved organic matter in seawater. Mar. Chem. 37, 191–221.

Coble, P.G., Green, S.A., Blough, N.V., Gagosian, R.B., 1990. Characterization of dissolved organic matter in the Black Sea by fluorescence spectroscopy. Nature, 348, 432–435.

Coble, P.G., 1996. Characterization of marine and terrestrial DOM in seawater using excitation-emission matrix spectroscopy. Mar. Chem. 51, 325–346.

Coble, P.G., 2007. Marine optical biogeochemistry: the chemistry of ocean color. Chem. Rev,107, 402–418.

Del Castillo, C.E., Coble, PG., Morell, JM., López, JM., Corredor, JE., 1999. Analysis of the optical properties of the Orinoco River plume by absorption and fluorescence spectroscopy. Mar. Chem. 66, 35–51.

Determann, S., Reuter, R., Willkomm, R., 1996. Fluorescence matter in the eastern Atlantic Ocean: Part 2. Vertical profiles and relation to water masses. Deep-Sea Res. 43, 345–360.

Dittmar, T., and Kattner, G., 2003. The biogeochemistry of the river and shelf ecosystem of the Arctic Ocean: A review. Marine Chemistry 83:103–120.

Ducklow, H, and Harris, R. 1993. Introduction to the JGOFS North Atlantic bloom experiment. Deep-Sea Res. 40, 1–8.

Flugister, FL., 1960. Atlantic Ocean Atlas of Temperature and Salinity Profiles and Data from the International Geophysical Year of 1957-1958. Atlas Series, Woods Hole Oceanographic Institution, Vol. 1.

Hansell, D.A., Carlson, C.A., Repeta, D.J., Reiner, S., 2009. Dissolved organic matter in the ocean: New insights stimulated by a controversy. Oceanography 22: 52–61, doi:10.5670/oceanog. 2009.109

Hansell, D.A. 2013. Recalcitrant Dissolved Organic Carbon Fractions. Annu. Rev. Mar. Sci. 2013. 5:3.1–3.25

Hayase, K., Tsubota, H., Sunada, I., 1989. Relationships of fluorescence and AOU in three north Pacific water samples. The Science of the total environment, 81/82, 315–318.

Hayase, K., and Shinozuka, N., 1995. Vertical distribution of fluorescent organic matter along with AOU and nutrients in the equatorial Central Pacific. Mar. Chem. 48, 283–290.

Ito, T., Follows, M.J., Boyle, E.A., 2004. Is AOU a good measure of respiration in the oceans? Geophysical Research Letters 31, 17305–17305.

Jackett T.R., McDougall T.J. 1997. A neutral density variable for the world's ocean. *J. Phys. Oceanogr.* 27: 237–263.

Jiao, N., Herndl, G. J., Hansell, D. A., Benner, R., Kattner, G., Wilhelm, S. W., Kirchman, D. L., Weinbauer, M. G., Luo, T., and Chen, F., 2010. Microbial production of recalcitrant dissolved organic matter: long-term carbon storage in the global ocean, Nat. Rev. Microbiol., 8, 593–599.

Jϕrgensen,L., Stedmon, C.A., Kragh, T., Markager, S., Middelboe, M., Sϕndergaard, M., 2011. Global trends in the fluorescence characteristics and distribution of marine dissolved organic matter. Mar. Chem. 126, 139–148.

Karstensen, J., Stramma, L., Visbeck, M., 2008. Oxygen minimum zones in the eastern tropical Atlantic and Pacific oceans. Progress in Oceanography 77, 331–350.

Kramer, G. D., and G. J. Herndl. 2004. Photo- and bioreactivity of chromophoric dissolved organic matter produced by marine bacterioplankton. Aquat. Microb. Ecol. 36: 239–246.

Lappo, S.S., Lozovatsky, I.D., Morozov, E.G., Sokov, A.V., Shapovalov, S.M., 2001. Variability of water structure in the Equatorial Atlantic. Dokl. – Earth Sci. Sect. 379: 739–743.

Lawaetz, A.J., and Stedmon, C.A., 2009. Fluorescence intensity calibration using the Raman scatter peak of water. Applied Spectroscopy 63(8), 936–940.

Legendre, P. and Legendre, L., 1998. Numerical Ecology. Number 20 in Developments in Environmental Modelling. Elsevier, Amsterdam, 2nd edition.

Logan, M., 2010. Biostatistical Design and Analysis Using R. A Practical Guide. Wiley-Blackwell, Oxford, UK. ISBN 978-1-4443-3524-8. 546 pp.

Machín, F., and Pelegrí, J. L., 2009. Northward penetration of Antarctic Intermediate Water off northwest Africa. Journal of Physical Oceanography, 39, 512-535.

Mamayev, O.I, 1975. Temperature-salinity analysis of world ocean waters, Elsevier Scientific, Amsterdam-Oxford-New York, 374 p.

McDougall, T.J. and Barker, P. M., 2011. Getting started with TEOS-10 and the Gibbs Seawater (GSW) Oceanographic Toolbox, 28 pp., SCOR/IAPSO WG127, ISBN 978-0-646-55621-5.

Mopper, K., Zhou, X., Kieber, R.J., Kieber, D.J., Sikorski, R.J., Jones, R.D., 1991. Photochemical degradation of dissolved organic carbon and its impact in oceanic carbon cycle. Nature, 353, 60–62.

Nelson, N.B., Siegel, D.A., Carlson, C.A., Swan, C., Smethie, W.M., Khatiwala, S., 2007. Hydrography of chromophoric dissolved organic matter in the North Atlantic. Deep-Sea Research I 54, 710–731.

Nelson, N.B., Siegel, D.A., Carlson, C.A., Swan, C.M., 2010. Tracing global biogeochemical cycles and meridional overturning circulation using chromophoric dissolved organic matter. Geophys. Res. Lett. 37:L03610.

Nelson, N.B., & Siegel D.A., 2013: Global distribution and dynamics of chromophoric dissolved organic matter. Annual Review of Marine Science, 5, 447–476.

Nieto-Cid, M., Álvarez-Salgado, Gago, J., X.A., Pérez, F.F., 2005. DOM fluorescence a tracer for biogeochemical processes in a coastal upwelling system (NW Iberian Peninsula). Mar. Ecol. Prog. Ser. 297: 33–50

Nieto-Cid., M., Álvarez-Salgado, X.A., Pérez, F.F., 2006. Microbial and photochemical reactivity of fluorescent dissolved organic matter in a coastal upwelling system. Limnol. Oceanogr. 51, 1391–1400.

Oudot, C., 1993. Carbon Data Obtained during the R/V L'Atalante cruise in the Atlantic Ocean (WOCE Section A07, 13 February–19 March 1993) http://cdiac.ornl.gov/ftp/oceans/a07woce/, Carbon Dioxide Information Analysis Center, Oak Ridge National Laboratory, US Department of Energy, Oak Ridge, Tennessee, doi:10.3334/CDIAC/otg.WOCE A07 1993, 1993b.

Orsi, A. H., Johnson, G. C., and Bullister, J. L., 1999. Circulation, mixing, and production of Antarctic Bottom Water, Prog. Oceanogr., 43, 55–109.

Romera-Castillo, C., Sarmento, H., Álvarez-Salgado, X.A., Gasol, J.M., Marrasé, C., 2010. Production of chromophoric dissolved organic matter by marine phytoplankton. Limnol. Oceanogr., 55(1), 446–454.

Romera-Castillo, C., Nieto-Cid, M., Castro, C.G., Marrasé, C., Largier, J., Barton, E.D., Álvarez-Salgado, X.A., 2011a. Fluorescence: Absorption coefficient ratio - Tracing photochemical and microbial degradation processes affecting coloured dissolved organic matter in a coastal system. Marine Chemistry 125, 26–38.

Romera-Castillo, C., Sarmento, H., Álvarez-Salgado, X.A., Gasol, J.M., Marrasé, C., 2011b. Net production/consumption of fluorescent coloured dissolved organic matter by natural bacterial assemblages growing on marine phytoplankton exudates. Applied and Environmental Microbiology 77, 7490–7498.

R Core Team (2012). R: A language and environment for statistical computing. R Foundation for Statistical Computing, Vienna, Austria. ISBN 3-900051-07-0, URL http://www.R-project.org/. Accessed on 11 December 2012.

Salisbury, J., Vandermark, D., Campbell, J., Hunt, C., Wisser, D., Reul, N., Chapron, B., 2011. Spatial and temporal coherence between Amazon River discharge, salinity, and light absorption by colored organic carbon in western tropical Atlantic surface waters. J. Geophys. Res. 116, C00H02, doi: 10.1029/2011JC006989.

San Antolín, M.A., Pelegrí, J.L., Machín, F.J., Benítez, V., 2012. Inter decadal changes in stratification and double diffusion in a transatlantic section along 7.5^{o}N. Sci. Mar., 76S1, 189–207. ISSN:0214–8358.

Sarafanov, A.; Sokov, A., and Demidov, A., 2007. Water mass characteristics in the equatorial North Atlantic: A section nominally along 6.5ºN, July 2000. J. Geophys. Res. 112, C12023,doi:10.1029/2007JC004222.

Siedler, G., Zangenberg, N., Onken, R., Morlière, A., 1992. Seasonal changes in the tropical Atlantic circulation: Observation andsimulation of the Guinea Dome. J. Geophys. Res. 97: 703–7150.

Siegel, D., S. Maritorena, N. Nelson, D. Hansell, and M. Lorenzi-Kayser. 2002. “Global Distribution and Dynamics of Colored Dissolved and Detrital Organic Materials.” Journal of Geophysical Research 107: 3228.

Stedmon, C.A., and Markager, S., 2005. Resolving the Variability in Dissolved Organic Matter Fluorescence in Temperate Estuary and its Catchment Using PARAFAC Analysis. Limnol. Oceanogr. 50, 686–697.

Schlitzer, R., Ocean Data View, http://odv.awi.de, 2011.

Stramma, L., Schott., F., 1999. The Mean Flow Field of the Tropical Atlantic Ocean. DeepSea Research II, 46, 279–303.

Stramma, L., 2008. Expanding Oxygen–Minimum Zones in the Tropical Oceans. Science, 320, 655.

Talley, L.D., Pickard, G.L., Emery, W.J., Swift, J.H., 2011. Descriptive Physical Oceanography: An Introduction (Sixth Edition), Elsevier, Boston, 560 pp.

Yamashita, Y., Tsukasaki, A., Nishida, T., Tanoue, E., 2007. Vertical and horizontal distribution of fluorescence dissolved organic matter in the Southern Ocean. Marine Chemistry 106, 498–509.

Yamashita, Y., and Tanoue, E., 2008. Production of bio-refractory fluorescent dissolved organic matter in the ocean interior. Nature 1, 579–582.

Yamashita, Y., R. M. Cory, J. Nishioka, K. Kuma, E. Tanoue, R. Jaffé (2010) Fluorescence characteristics of dissolved organic matter in the deep waters of the Okhotsk Sea and the northwestern North Pacific Ocean, Deep Sea Research Part II: Topics in Oceanography, 57: 1478-1485. doi:10.1016/j.dsr2.2010.02.016.

Weiss, R.F., 1970. The solubility of nitrogen, oxygen and argon in water and seawater. Deep-Sea Research 17, 721–735.

WOCE, 1994. WOCE Operations Manual: Vol. 3, Sect. 3.1, Part 3.1.3: WHP Operations and Methods Oxygen determination. Rev. 1, Nov. 1994. Woods Hole, MA, USA, 12 pp.

Zuur A.F., Ieno E.N., Walker N.J., Saveliev A.A., Smith G.M., 2009. Mixed Effects Models and Extensions in Ecology with R. Springer, New York: 574 pp.

Warton, D. I., Duursma, R. A., Falster, D. S., and Taskinen, S., 2012. Smatr 3 - an R package for estimation and inference about allometric lines. Methods in Ecology and Evolution, 3, 257–259.

Tables

Table 1. F(340/440) - AOU linear relationships as obtained from the model II regression (SMA technique, see Methods). These relationships are determined for the ocean surface (0 - 200 m) and ocean interior (deeper than 200 m), and for the different water strata (central, intermediate, deep and bottom waters) of the ocean interior. The water strata are characterized using the neutral density criteria (see Methods).

Table 2. Result from the ANCOVA analysis. Slope for the linear relationship between ΔF(340/440) and ΔAOU among water strata using model II regression type SMA. The relationships are evaluated through the correlation coefficient, R^2, and the significance p-value (α = 0.05). The existence of differences between the calculated slopes for each water strata with the general slope of $3.14\ (\pm 0.08)\times 10^{-5}$ is evaluated using the statistic test of Likelihood ratio and the p-value.

Figures

Fig. 1. Study area showing the stations used in this study along 7.5ºN, occupied during the MOC2-Equatorial cruise.

Fig. 2. Colour contour maps for (a) potential temperature, θ (ºC), (b) salinity, and (c) dissolved oxygen, O^2 (μmol kg^{-1}) for the 7.5ºN line. Black lines represent neutral density, γ^n, isolines separating the water strata: central waters (SACW and NACW, $26.65 < \gamma^n < 27.3$), intermediate waters (AAIW, $27.3 < \gamma^n < 27.8$), deep waters (NADW, $27.8 < \gamma^n < 28.12$) and bottom waters (AABW, $\gamma^n > 28.12$).

Fig. 3. Vertical profiles for (a) potential temperature θ (ºC), (b) salinity and (c) dissolved oxygen, O^2 (μmol kg^{-1}). Vertical profiles are in different grey shades as a function of longitude (ºW). A reference profile (red curve) is calculated as a zonal average at each depth level. (d) θ/S diagram of 7.5ºN line for the ocean interior (waters deeper than 200 m), color-coded for dissolved oxygen, O^2 (μmol/kg); dotted lines represent the isoneutrals separating the water strata: central waters (SACW and NACW, $26.65 < \gamma^n < 27.3$), intermediate waters (AAIW, $27.3 < \gamma^n < 27.8$), deep waters (NADW, $27.8 < \gamma^n < 28.12$) and bottom waters (AABW, $\gamma^n > 28.12$).

Fig. 4. Contour maps for (a) fluorescence intensity, F(340/440) (R.U.) and (b) Chl-a (mg m^{-3}), from the sea surface down to 250 m depth. Black lines represent AOU isolines. Black triangles are sub-surface maximum values for F(340/440) (R.U.). Black dots are sub-surface maximum values for Chl-a (mg $m\text{-}^3$).

Fig. 5. Vertical profiles of (a) F(340/440) (R.U.) and (b) AOU (μmol kg^{-1}), with different grey as a function of longitude (ºW). A reference profile (red curve) is calculated as a zonal average at each depth level.

Fig. 6. Contour maps of (a) fluorescence intensity, F(340/440) (R.U.) and (b) AOU (μmol kg^{-1}) , along 7.5ºN. Black lines represent neutral density, γ^n, isolines. Those isoneutrals delimiting the different water strata for the ocean interior are shown: central waters (SACW and NACW, $26.65 < \gamma^n < 27.3$), intermediate waters (AAIW, $27.3 < \gamma^n < 27.8$), deep waters (NADW, $27.8 < \gamma^n < 28.12$) and bottom waters (AABW, $\gamma^n > 28.12$).

Fig. 7. θ/S diagram for the ocean interior, color-coded for F(340/440) (a) and (b) AOU. Dotted lines represent the isoneutrals separating the water strata: central waters (SACW and NACW, $26.65 < \gamma^n < 27.3$), intermediate waters (AAIW, $27.3 < \gamma^n < 27.8$), deep waters (NADW, $27.8 < \gamma^n < 28.12$) and bottom waters (AABW, $\gamma^n > 28.12$).

Fig. 8. Property-property plots for the ocean interior (waters deeper than 200 m) for (a) F(340/440) (R.U.) versus AOU (μmol kg^{-1}) and (b) ΔF(340/440) (R.U.) versus ΔAOU (μmol kg^{-1}). The regression equation is $\Delta F(340/440) = 3.14 (\pm 0.08) \times 10^{-5} \times \Delta AOU$ with $R^2 = 0.79$, $p < 0.001$. Water strata are distinguished by neutral density surfaces. Central waters (SACW, NACW, $26.65 < \gamma^n < 27.3$) represented by red triangles, intermediate waters (AAIW, $27.3 < \gamma^n < 27.8$) represented by green triangles, deep waters (NADW, $27.8 < \gamma^n < 28.12$) represented by black dots, and bottom waters (AABW, $\gamma^n > 28.12$) represented by blue dots.

Fig. 9. Contour maps of (a) F(340/440) (black isolines) and ΔF(340/440) (R.U.)(colour filled contour) and (b) AOU (black isolines) and ΔAOU (μmol kg^{-1}) (colour filled contour).

Table

Table 1. F(340/440) - AOU linear relationships as obtained from the model II regression (SMA technique, see Methods). These relationships are determined for the ocean surface (0 - 200 m) and ocean interior (deeper than 200 m), and for the different water strata (central, intermediate, deep and bottom waters) of the ocean interior. The water strata are characterized using the neutral density criteria (see Methods).

Layer / Water strata	***Intercept ($\times 10^4$)***	***Slope ($\times 10^5$)***	***R^2***	***n***	***p***	***SD F(340/440) ($\times 10^4$)***	***SD AOU***
Surface (0-200m)	34 (±2)	5.41 (±0.17)	0.83	170	<0.001	±0.4	±68.2
Ocean interior (>200m)	89 (±1)	1.20 (±0.01)	0.05	360	<0.001	±6.4	±52.8
Central w. (NACW/SACW) $26.65 < \gamma^n < 27.3$	50 (±2)	3.07 (±0.14)	0.81	131	<0.001	±9.9	±31.3
Intermediate w. (AAIW) $27.3 < \gamma^n < 27.8$	73 (±4)	1.85 (±0.22)	0.07	102	< 0.05	±4.9	±26.4
Deep w. (NADW) $27.8 < \gamma^n < 28.12$	78 (±2)	3.60 (±0.31)	0.27	126	<0.001	±3.9	±10.6
Bottom w. (AAWB) $\gamma^n > 28.12$	—	—	< 0.01	30	0.814	±4.3	±10.2

Table 2. Result from the ANCOVA analysis. Slope for the linear relationship between ΔF(340/440) and ΔAOU among water strata using model II regression type SMA. The relationships are evaluated through the correlation coefficient, R^2, and the significance p-value (α = 0.05). The existence of differences between the calculated slopes for each water strata with the general slope of $3.14(\pm0.08)\times10^{-5}$ is evaluated using the statistic test of Likelihood ratio and the p-value.

Water strata	*Slope (×10^5)*	R^2	*p*	*Likelihood statistic*	*p*
General	3.14(± 0.08)	0.79	< 0.001	-	-
Central	2.9 ± 0.1	0.92	< 0.001	r_{98} = - 0.32	< 0.05
Intermediate	3.1 ± 0.1	0.79	< 0.001	r_{100} = - 0.05	0.58
Deep	4.7 ± 0.3	0.57	< 0.001	r_{124} = 0.55	< 0.001
Bottom	9.5 ± 2.2	0.25	< 0.05	r_{28} = 0.84	< 0.001

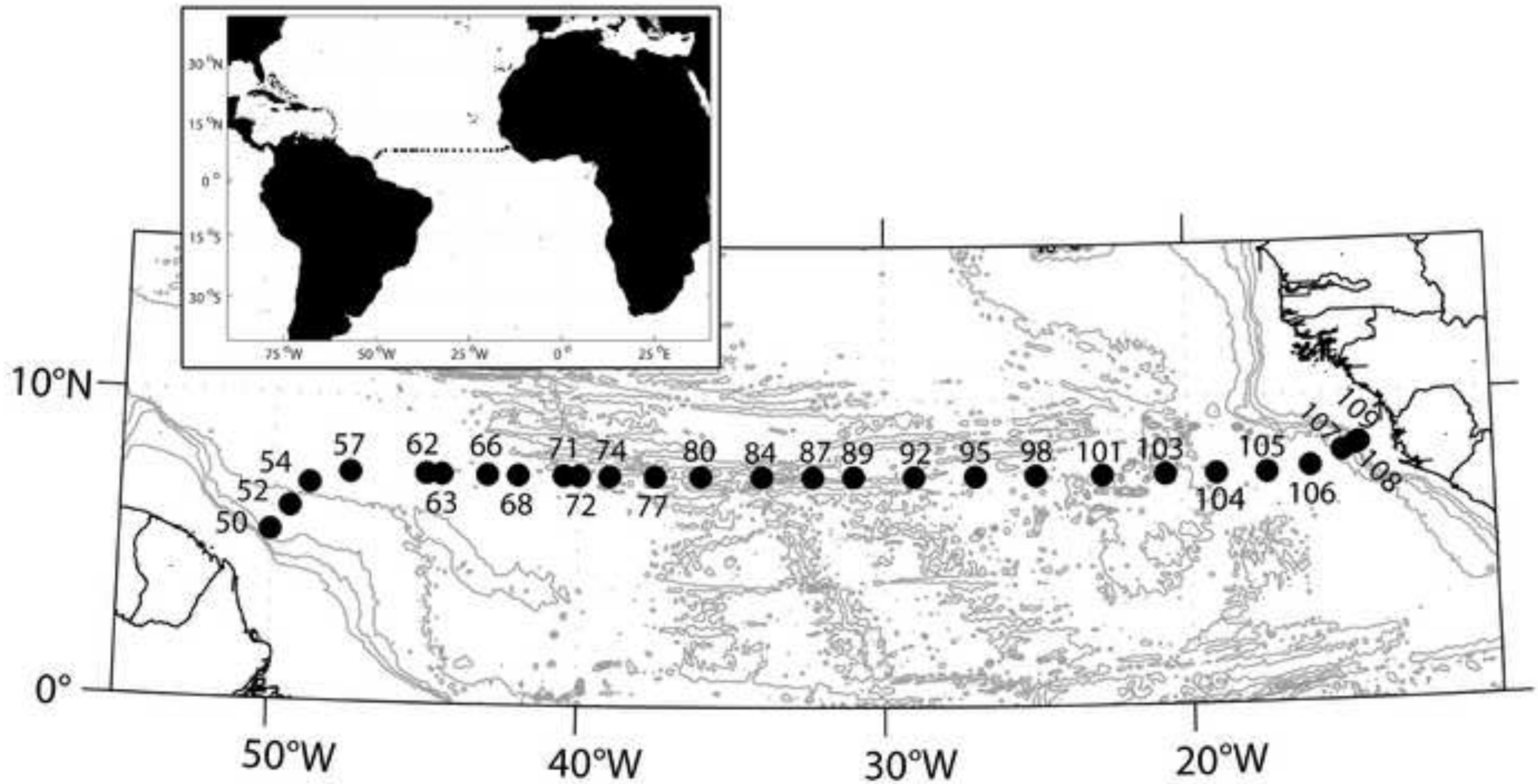

30 °N
15 °N
0 °
15 °S
30 °S
75 °W
50 °W
25 °W
0 °
25 °E
10°N
0°
50°W
40°W
30°W
20°W
50
52
54
57
62
63
66
68
71
72
74
77
80
84
87
89
92
95
98
101
103
104
105
106
107
108
109

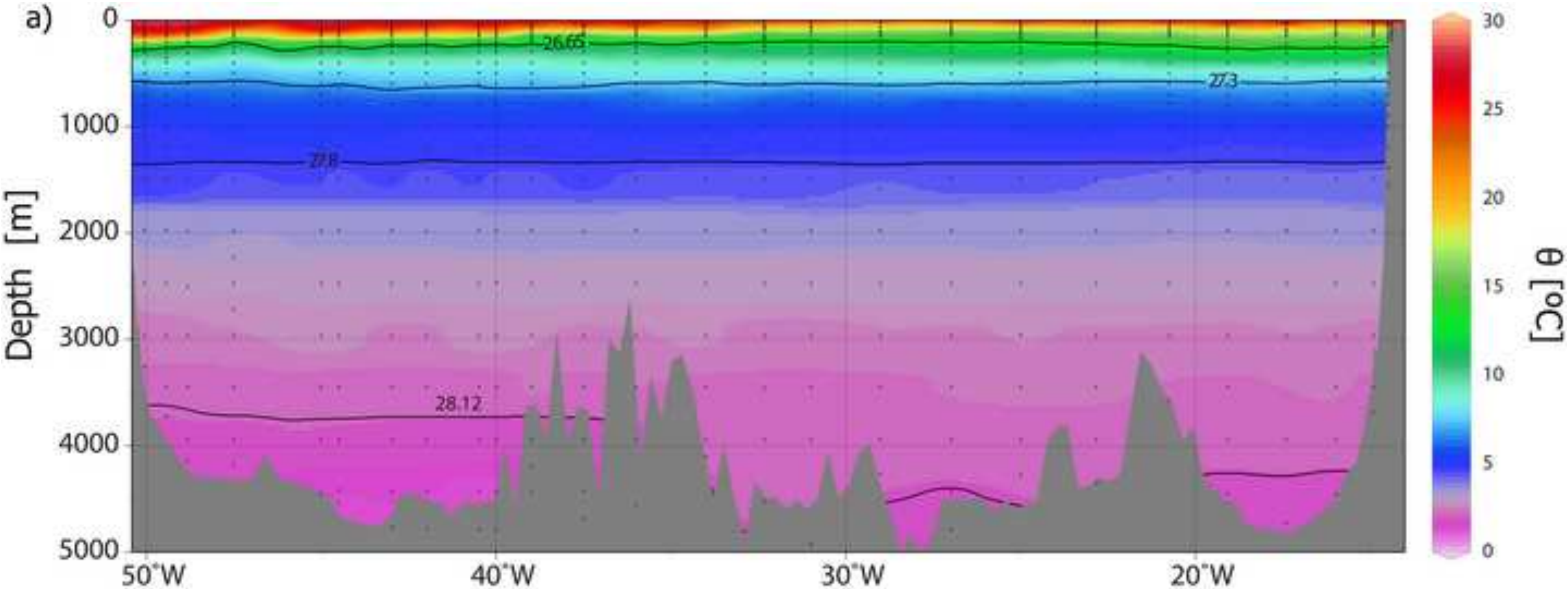

a)
Depth [m]
0
1000
2000
3000
4000
5000
50˚W
40˚W
30˚W
20˚W
26.65
27.3
27.8
28.12
θ [ºC]
30
25
20
15
10
5
0

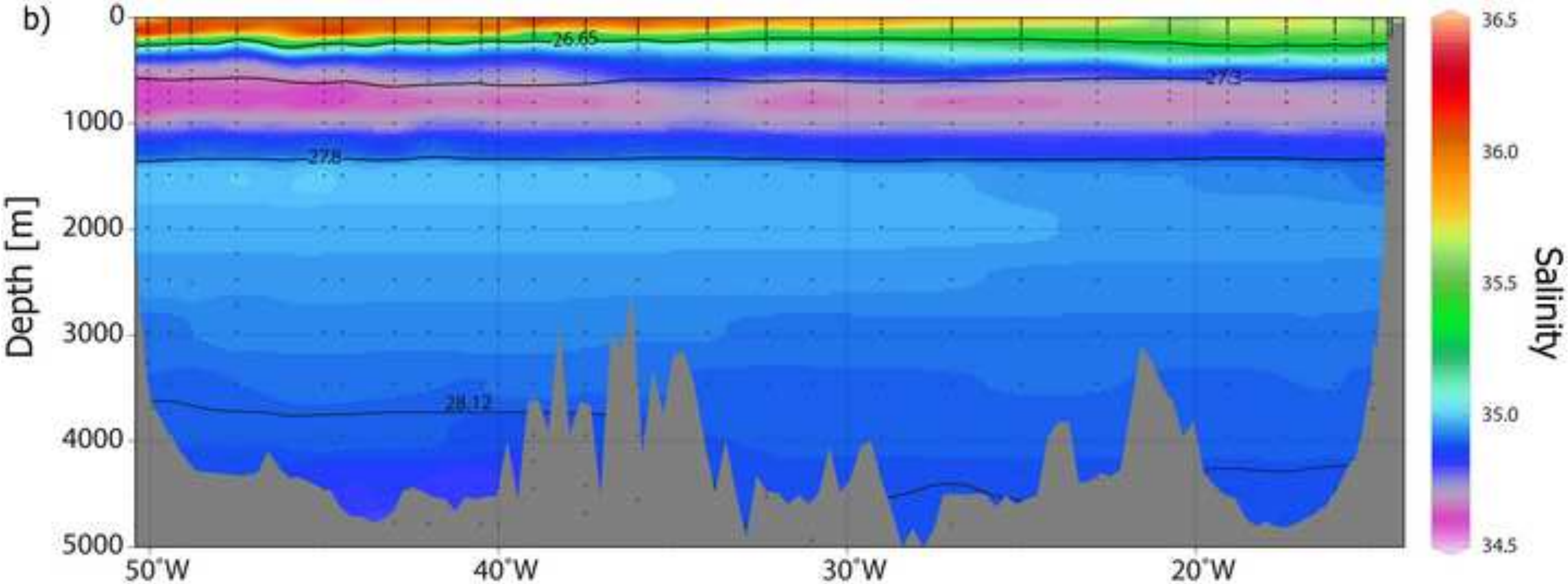

b)
0
1000
2000
3000
4000
5000
Depth [m]
50°W
40°W
30°W
20°W
26.65
27.3
27.8
28.12
36.5
36.0
35.5
35.0
34.5
Salinity

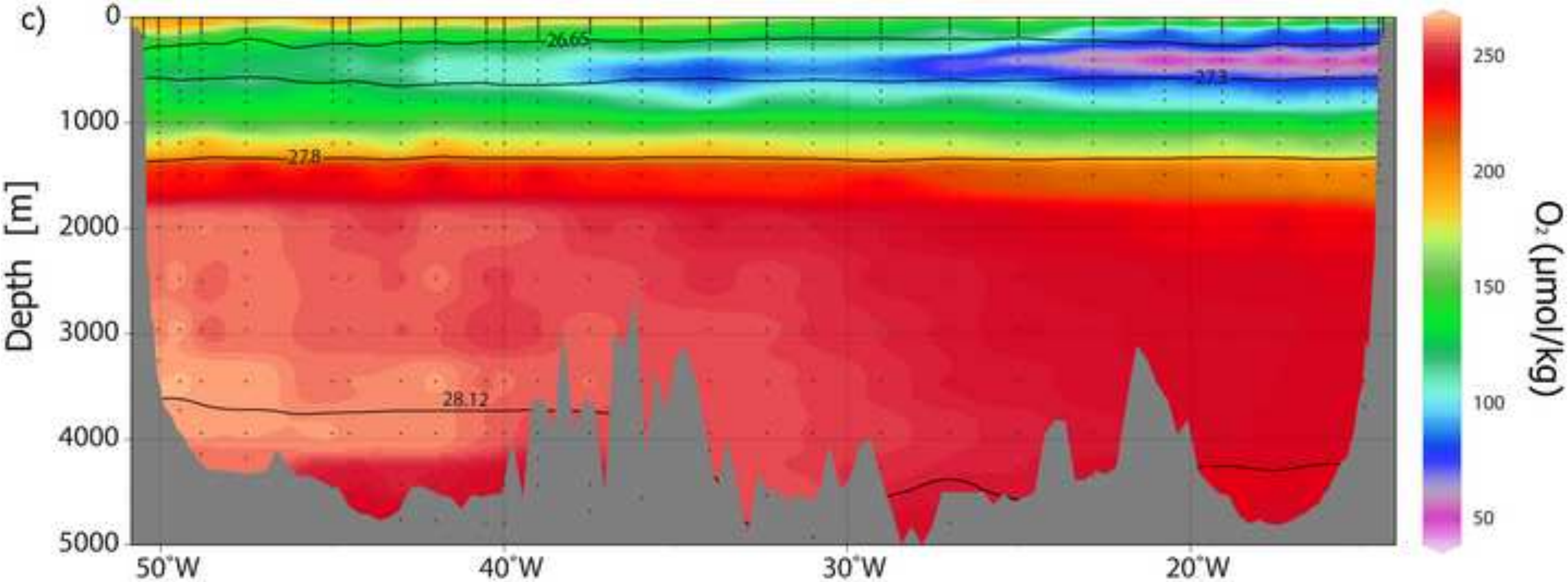

c)
Depth [m]
0
1000
2000
3000
4000
5000
50°W
40°W
30°W
20°W
26.65
27.3
27.8
28.12
O₂ (μmol/kg)
250
200
150
100
50

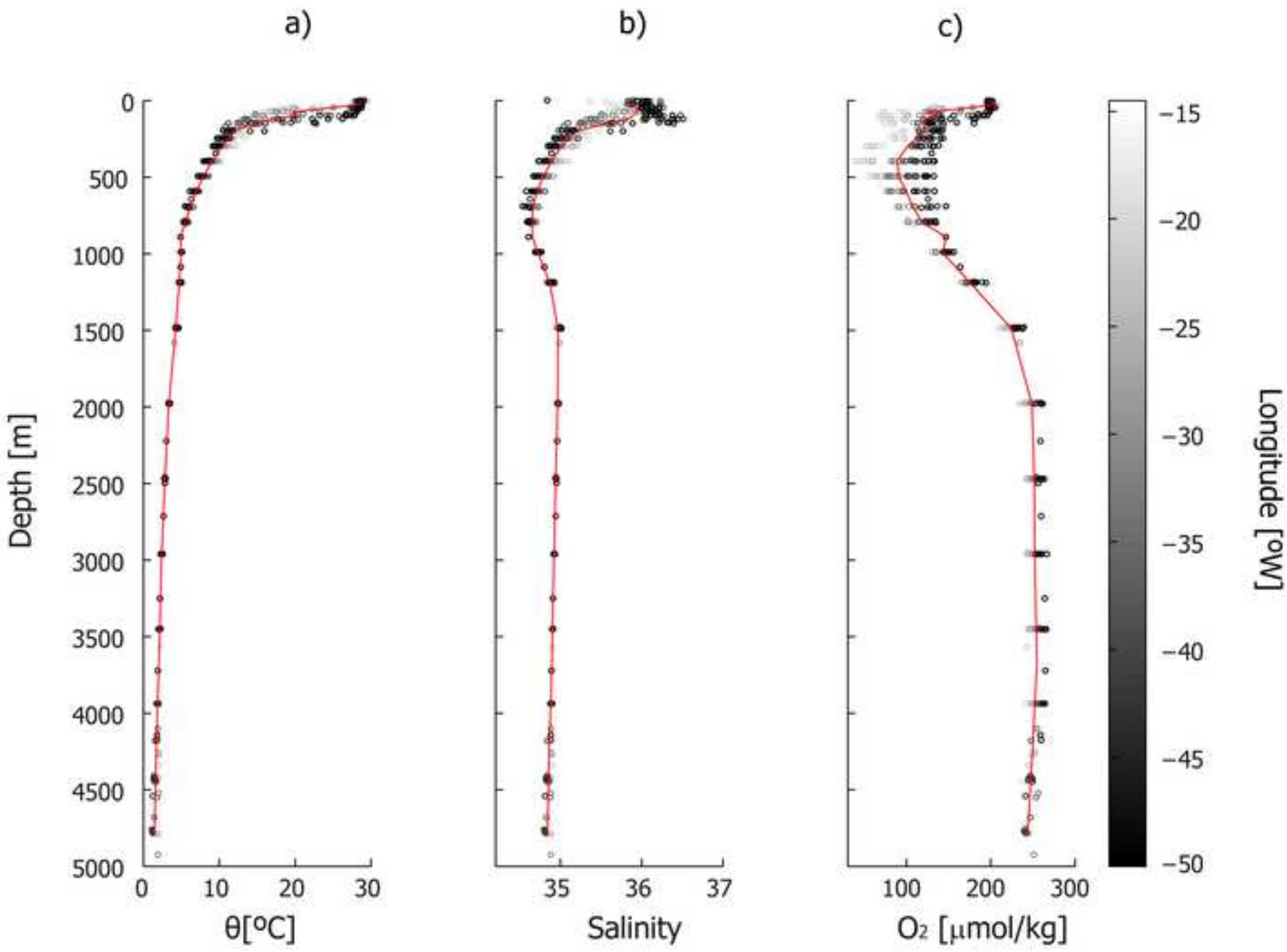

a)
b)
c)
Depth [m]
0
500
1000
1500
2000
2500
3000
3500
4000
4500
5000
0
10
20
30
θ[ºC]
35
36
37
Salinity
100
200
300
O2 [μmol/kg]
Longitude [ºW]
−15
−20
−25
−30
−35
−40
−45
−50

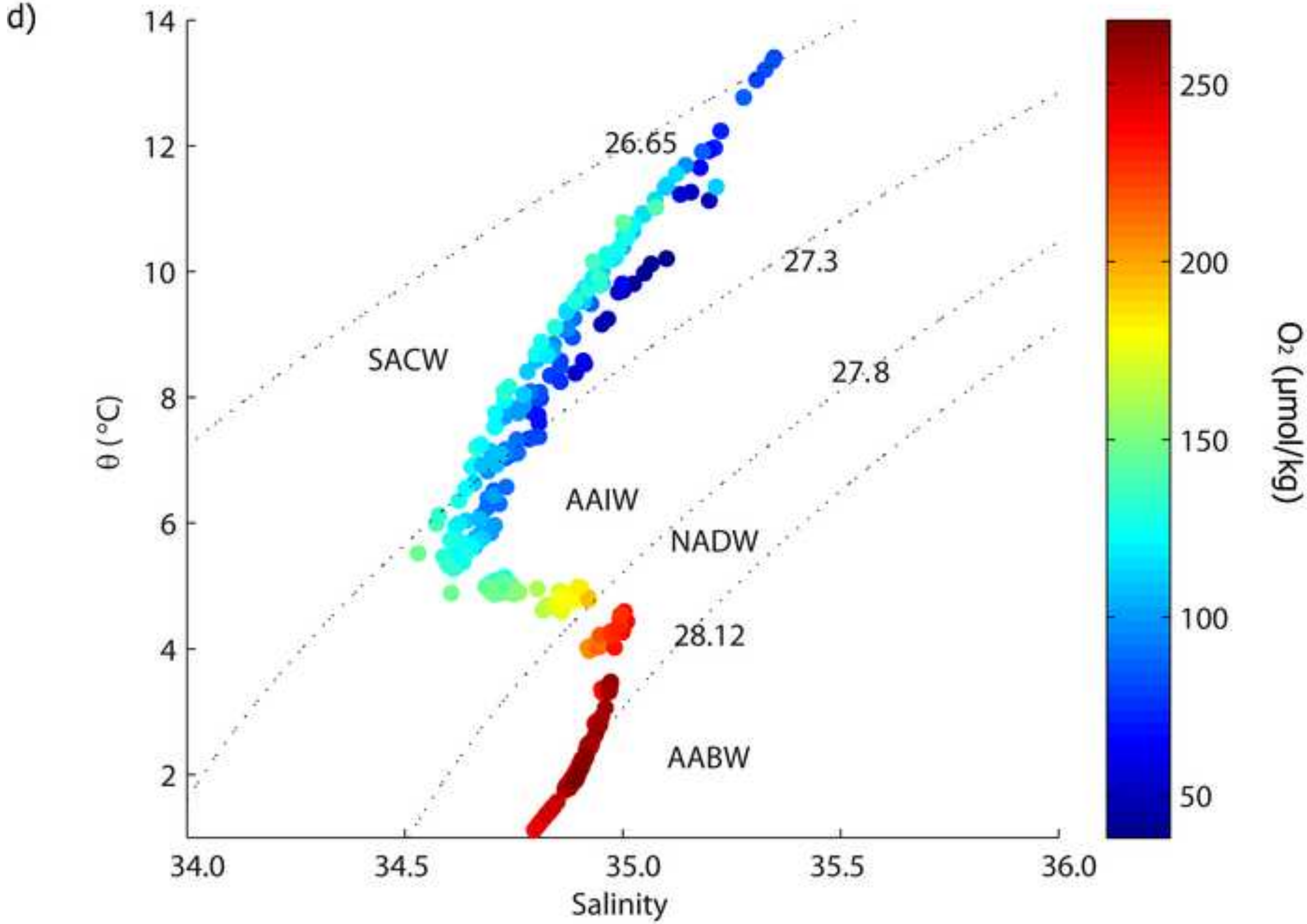
d)
14
12
10
8
6
4
2
θ (°C)
34.0
34.5
35.0
35.5
36.0
Salinity
26.65
27.3
27.8
28.12
SACW
AAIW
NADW
AABW
250
200
150
100
50
O₂ (μmol/kg)

a)

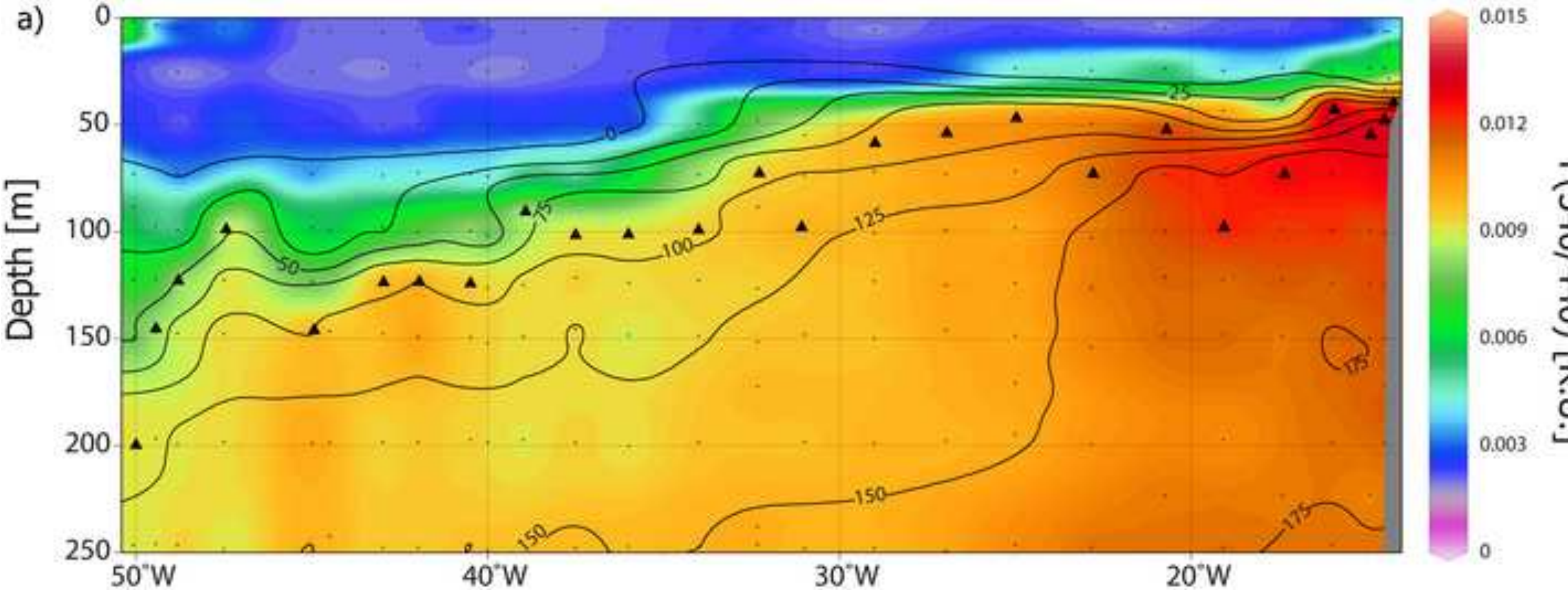

0
50
100
150
200
250
Depth [m]
50°W
40°W
30°W
20°W
0
25
50
75
100
125
150
175
0.015
0.012
0.009
0.006
0.003
0
F(340/440) [R.U.]

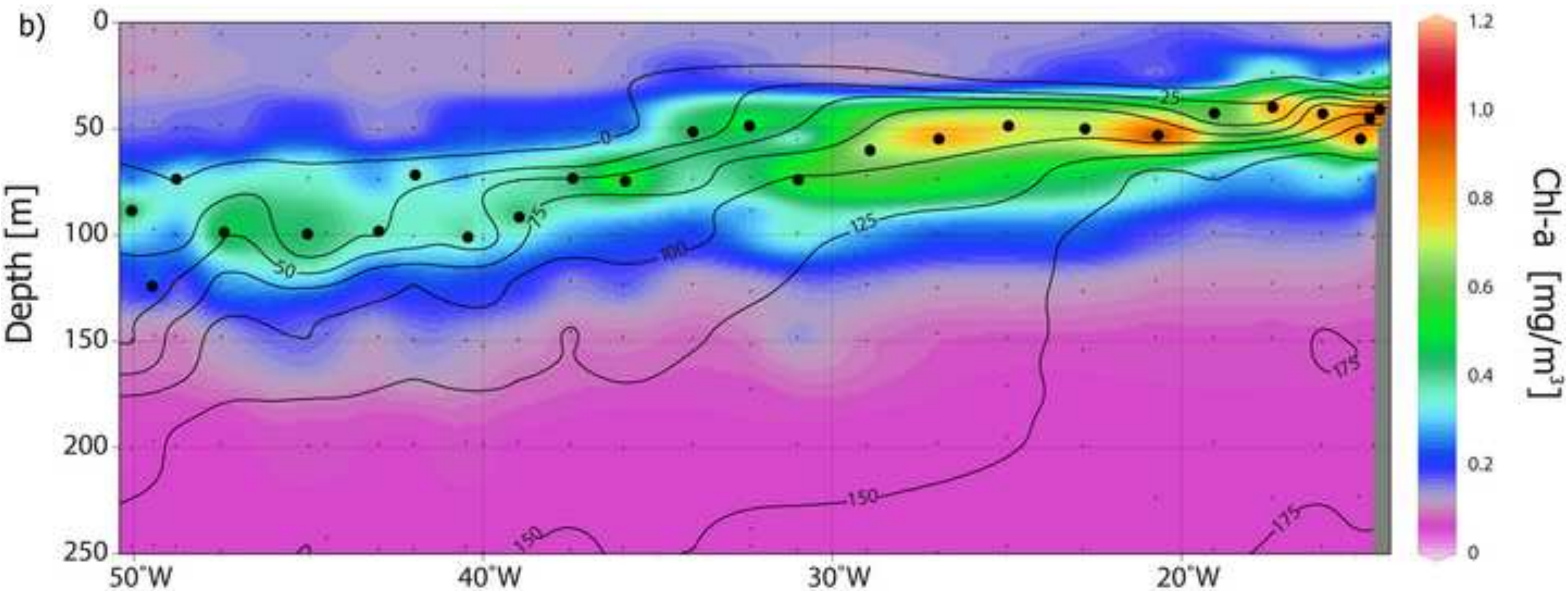
b)
Depth [m]
0
50
100
150
200
250
50°W
40°W
30°W
20°W
Chl-a [mg/m³]
1.2
1.0
0.8
0.6
0.4
0.2
0
0
25
50
75
100
125
150
175

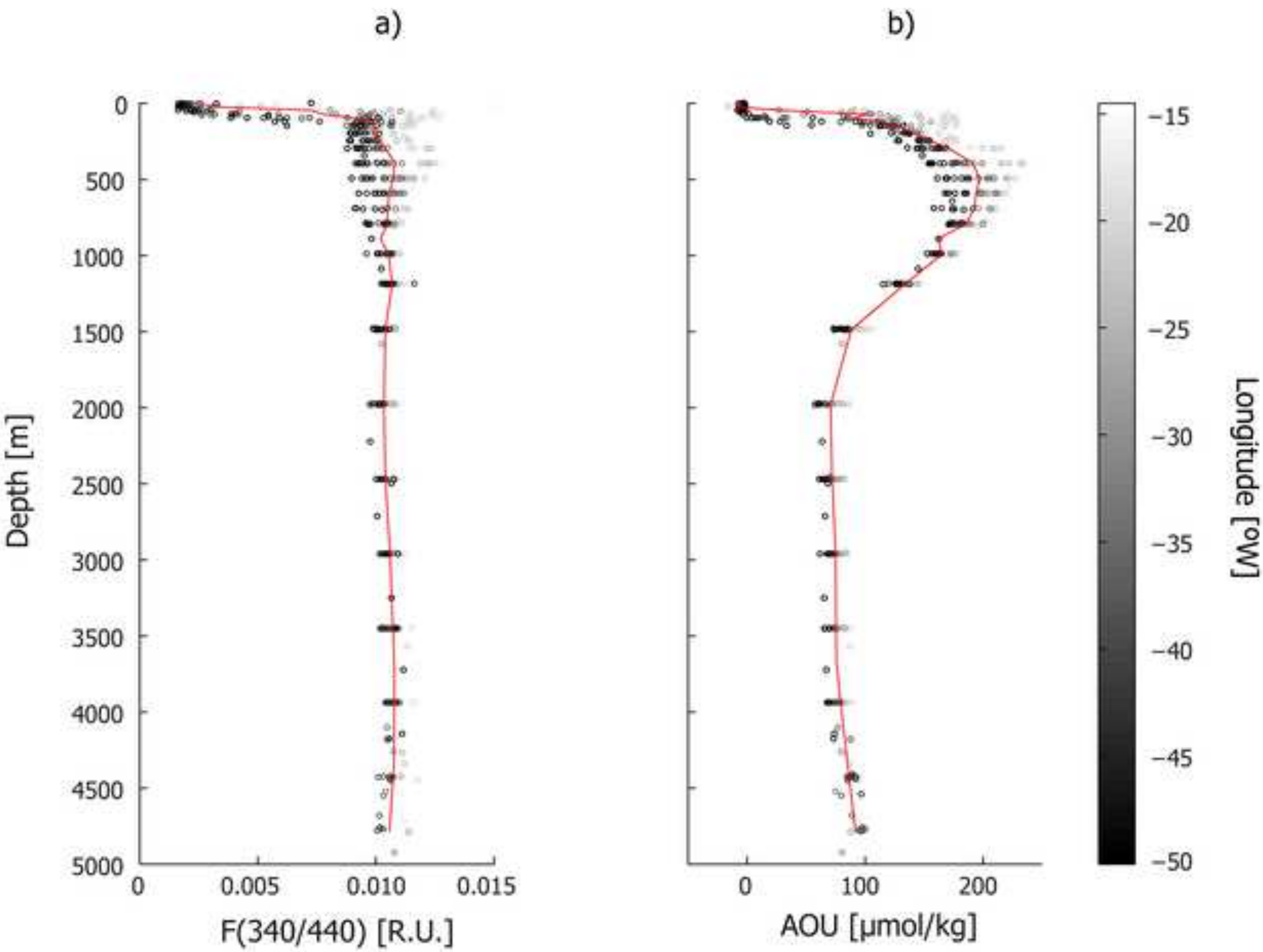

a)
b)
Depth [m]
0
500
1000
1500
2000
2500
3000
3500
4000
4500
5000
0
0.005
0.010
0.015
F(340/440) [R.U.]
0
100
200
AOU [µmol/kg]
Longitude [ºW]
−15
−20
−25
−30
−35
−40
−45
−50

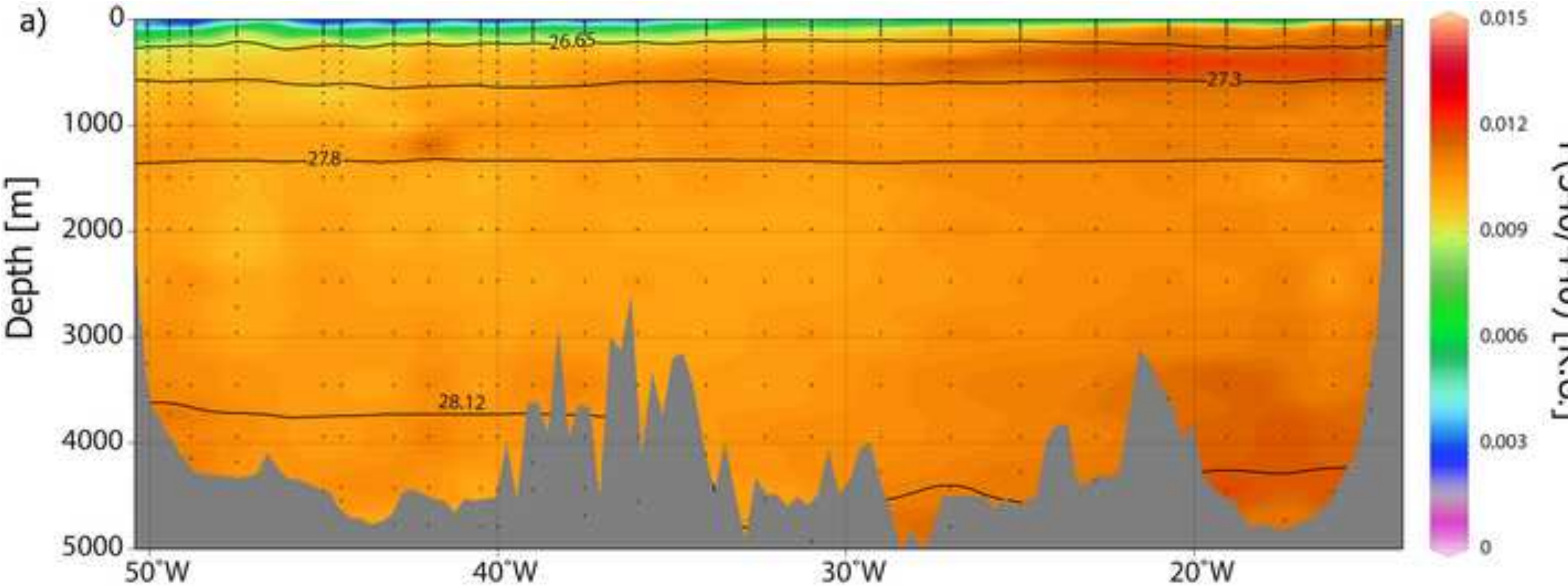

a)
Depth [m]
0
1000
2000
3000
4000
5000
50°W
40°W
30°W
20°W
26.65
27.3
27.8
28.12
F(340/440) [R.U.]
0.015
0.012
0.009
0.006
0.003
0

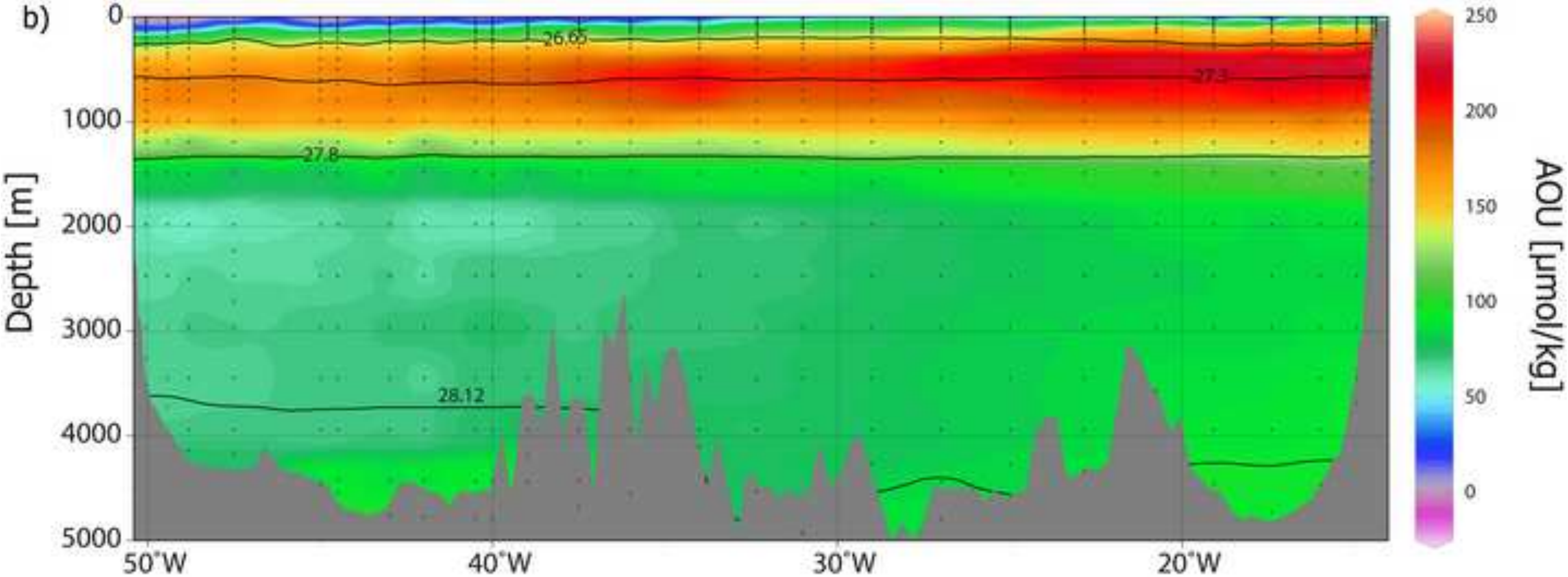
b)
0
1000
2000
3000
4000
5000
Depth [m]
26.65
27.3
27.8
28.12
50°W
40°W
30°W
20°W
250
200
150
100
50
0
AOU [µmol/kg]

a)

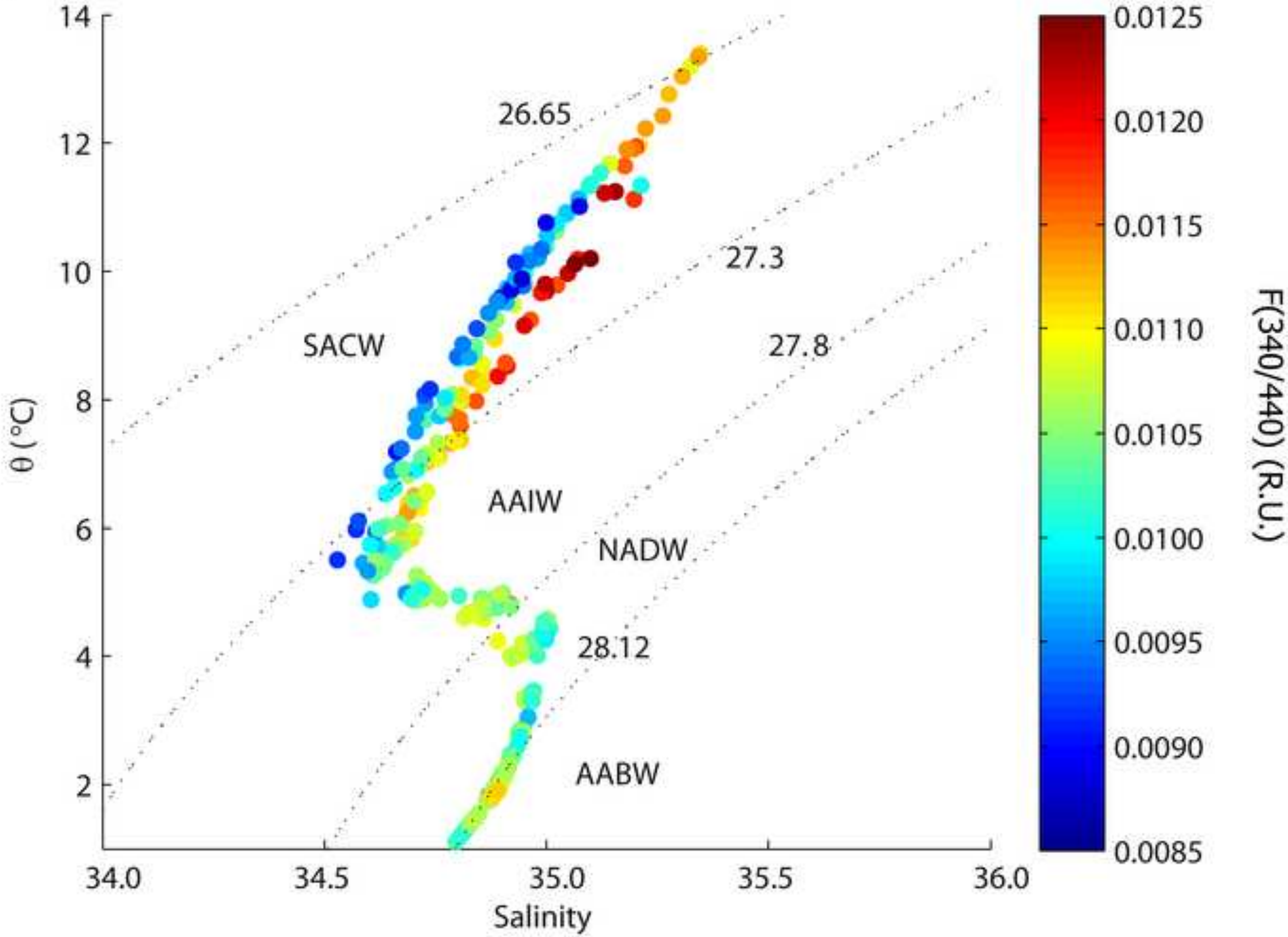
14
12
10
8
6
4
2
θ (°C)
34.0
34.5
35.0
35.5
36.0
Salinity
26.65
27.3
27.8
28.12
SACW
AAIW
NADW
AABW
0.0125
0.0120
0.0115
0.0110
0.0105
0.0100
0.0095
0.0090
0.0085
F(340/440) (R.U.)

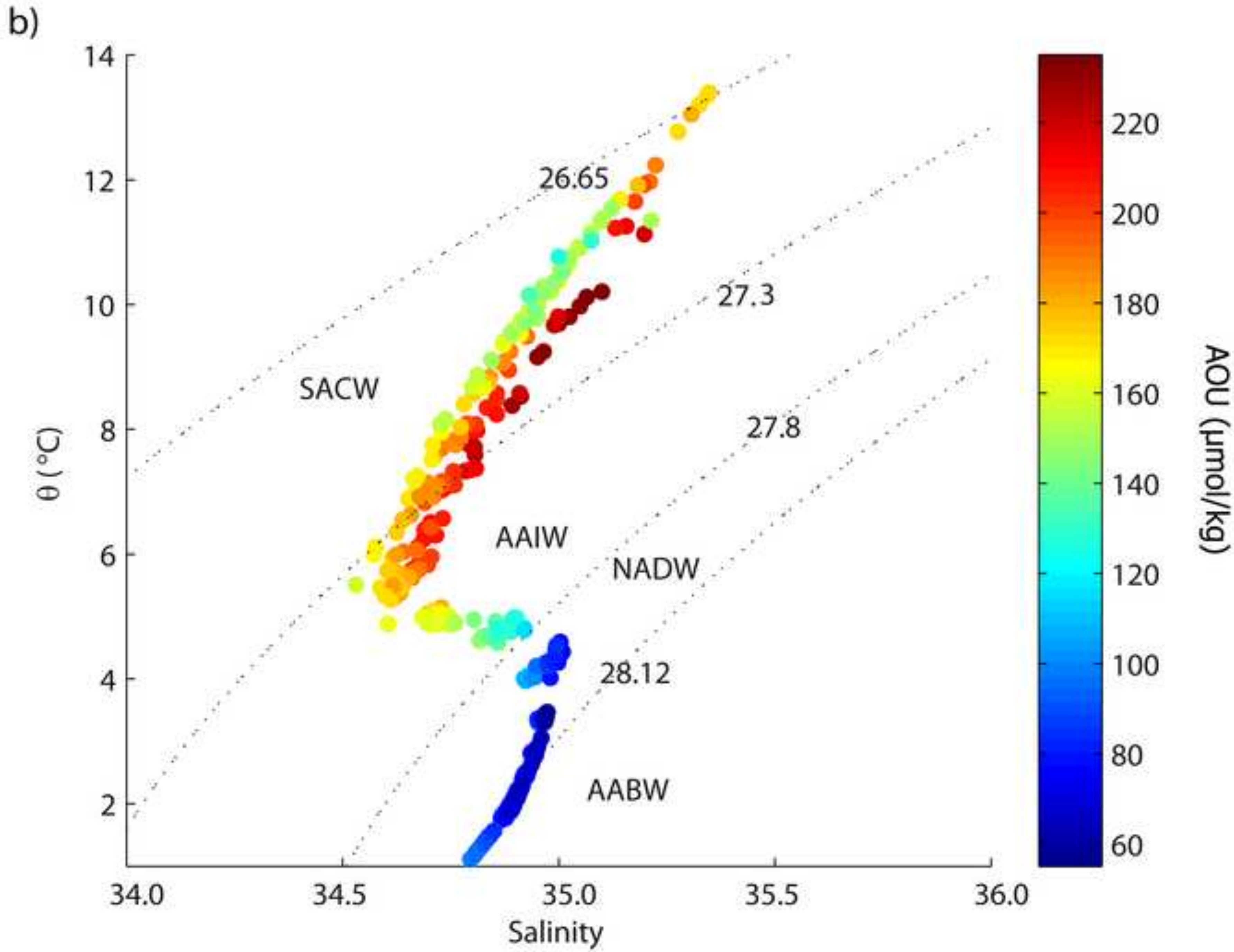
b)
14
12
10
8
6
4
2
θ (°C)
34.0
34.5
35.0
35.5
36.0
Salinity
26.65
27.3
27.8
28.12
SACW
AAIW
NADW
AABW
220
200
180
160
140
120
100
80
60
AOU (µmol/kg)

a)

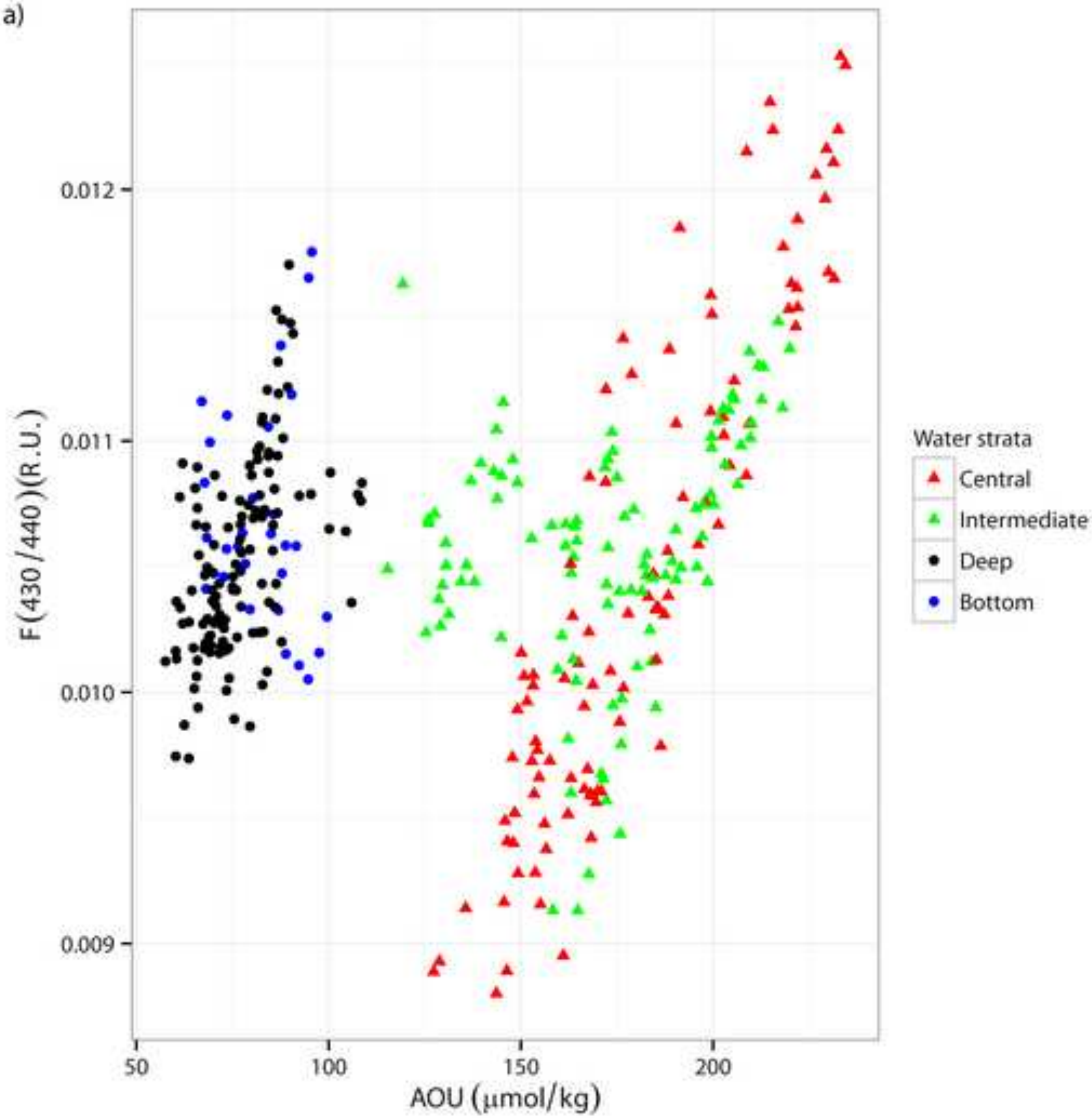

F(430/440)(R.U.)
0.012
0.011
0.010
0.009
50
100
150
200
AOU (μmol/kg)
Water strata
Central
Intermediate
Deep
Bottom

b)

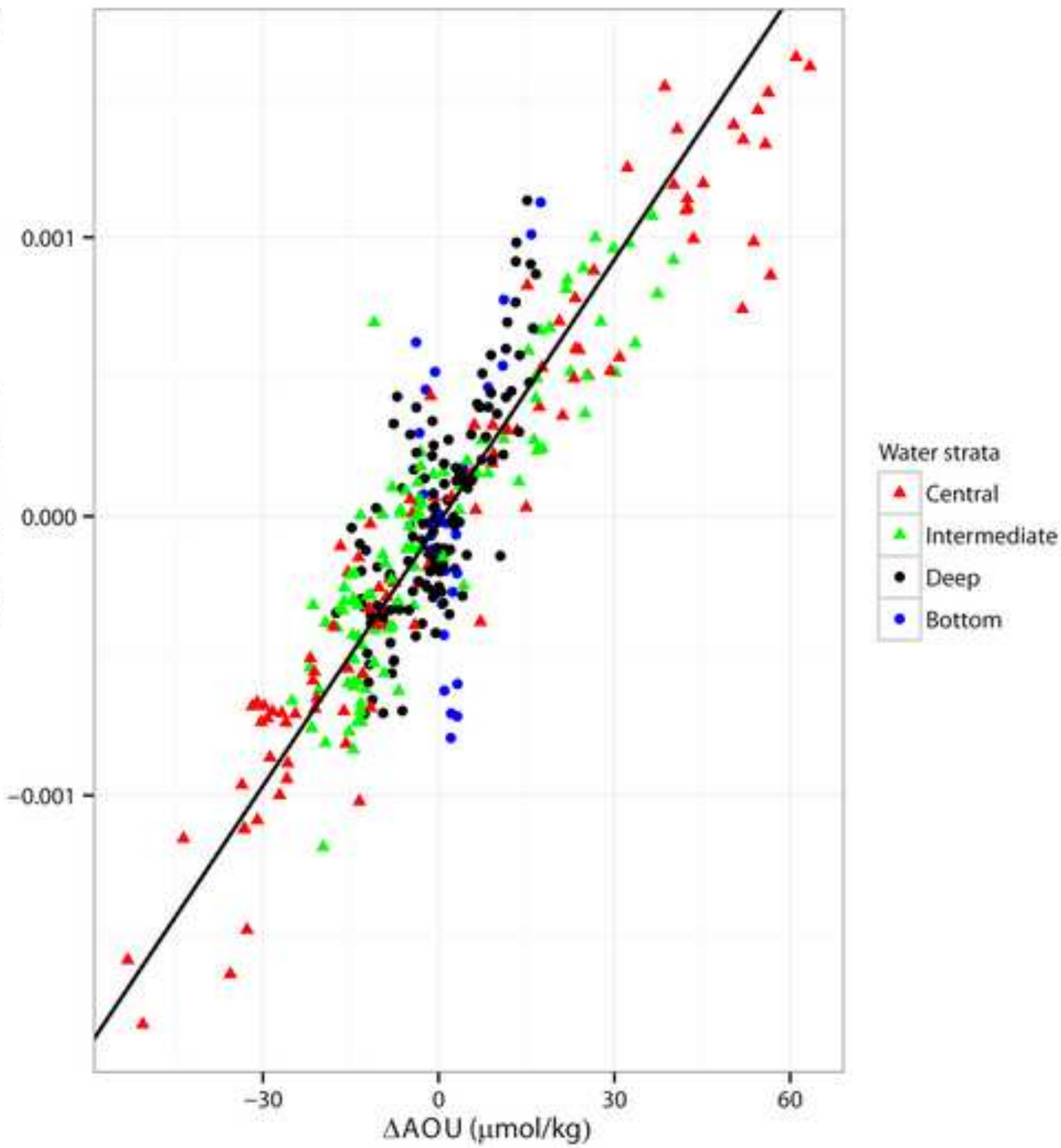

0.001
0.000
−0.001
ΔF(430/440) (R.U.)
−30
0
30
60
ΔAOU (μmol/kg)
Water strata
Central
Intermediate
Deep
Bottom

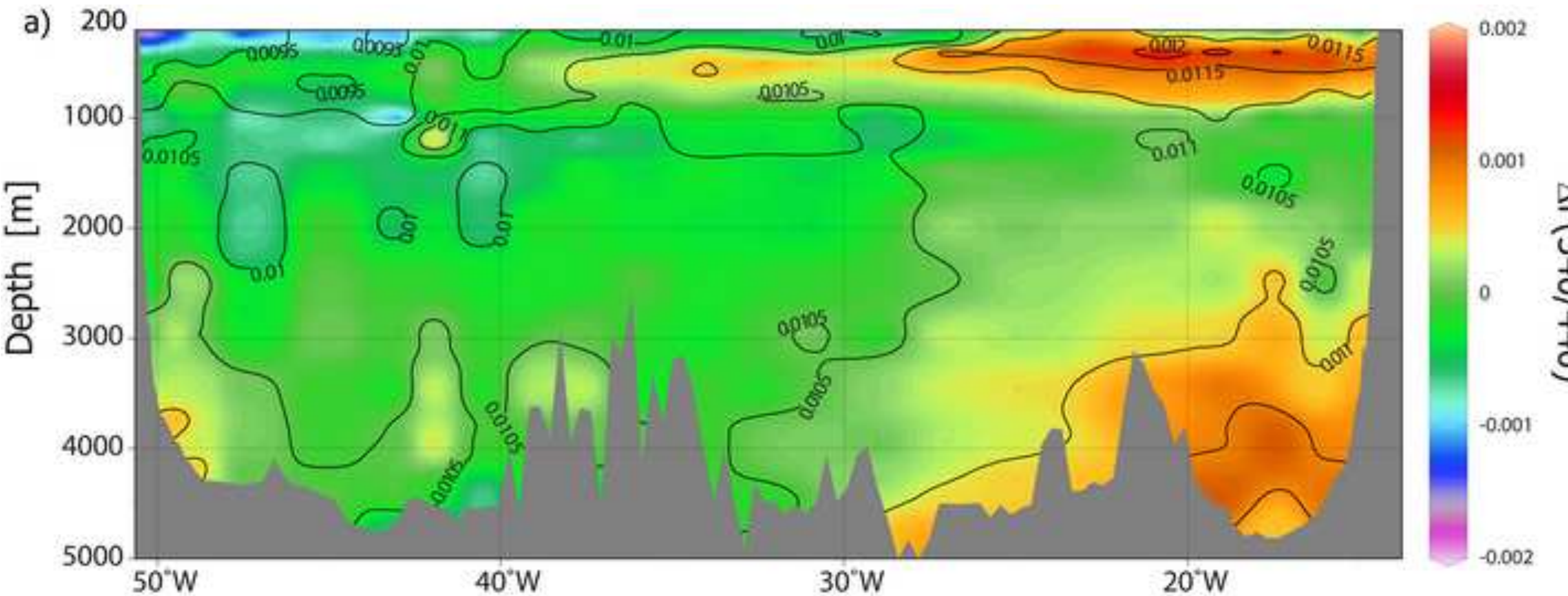

a)
Depth [m]
200
1000
2000
3000
4000
5000
50°W
40°W
30°W
20°W
ΔF(340/440)
0.002
0.001
0
-0.001
-0.002

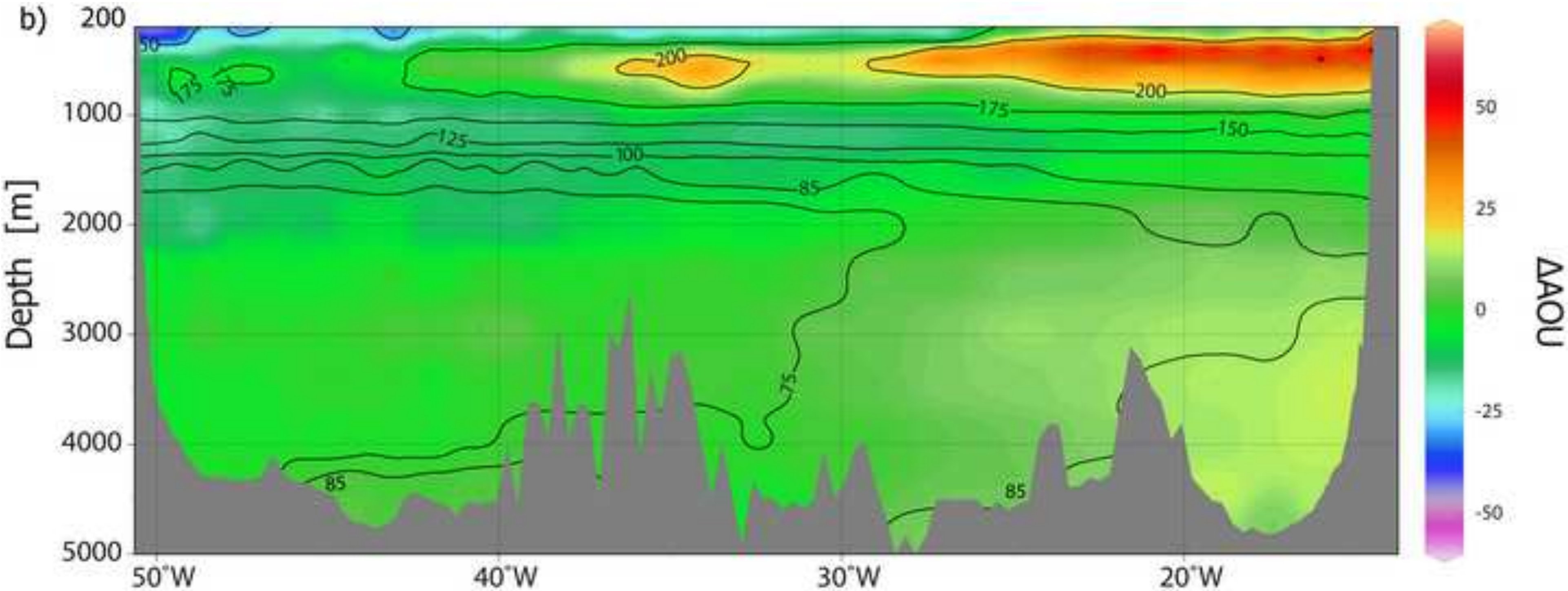

b)
200
1000
2000
3000
4000
5000
Depth [m]
50°W
40°W
30°W
20°W
50
200
175
150
125
100
85
75
50
25
0
-25
-50
ΔAOU